The Italian Seismic Hazard Model (ISHM): Objectives, Methodology, and Governance

A. Akinci, V. D'Amico, M. Taroni, G. Lanzano, G. Falcone, C. Chiarabba, A. Antonucci, R. Azzaro, R. Basili, M. M. C. Carafa, V. Convertito, G. Dalla Via, S. D'Amico, E. Giampiccolo, B. Lolli, F. E. Maesano, C. Mascandola, I. Munafò, C. Pandolfi, P. Roselli, A. Rovida, A. Scala, S. Sgobba, F. Sparacino, M. M. Tiberti, A. Tramelli, G. Tusa, T. Tuvè, F. Visini, *collaboration with GEM*

Istituto Nazionale di Geofisica e Vulcanologia (INGV), Italy

The Italian Seismic Hazard Model (ISHM) project is a two-year project, coordinated by the Seismic Hazard Center (CPS) of the Istituto Nazionale di Geofisica e Vulcanologia (INGV), aimed at delivering a new long-term, time-independent Probabilistic Seismic Hazard Assessment (PSHA) model for Italy by the end of 2026. The new model will update earlier national analyses - i.e., MPS04 (Stucchi et al., 2004) and MPS19 (Meletti et al., 2021) - and should serve as a scientific basis for future seismic regulations, territorial planning, and national risk-mitigation strategies. Developed within a methodological and transparent framework, the ISHM will integrate multidisciplinary data, state-of-the-art methodologies, and internationally aligned best practices in PSHA.

The ISHM project's governance relies on three complementary components: 1) the Project Team, responsible for scientific development, structured into five thematic units: Core Team, Seismicity Rate Model (SRM) Team, Ground Motion Model (GMM) Team, Hazard Calculation Team, and Model Testing Team; 2) the Advisory Panel (AP), composed of leading international experts who will provide scientific guidance, methodological review, and support in key decisions such as logic-tree construction; 3) the Strategic Stakeholder Group (SSG), including representatives from national engineering communities, and civil protection authorities who will ensure that model outputs, formats, and metrics are suitable for regulatory and operational applications. Throughout the project, structured interactions with members of the AP and SSG—through joint meetings, consultations, and workshops—will support the interpretation of preliminary results and contribute to strengthening both the scientific and technical components of the model. These exchanges could also help anticipating implications for seismic design codes and national risk-reduction policies, and ensuring a close connection between scientific development and operational needs.

The ISHM will integrate a suite of complementary SRMs based on updated input data (e.g., earthquake catalogues, fault databases, geodetic data, etc.), including area-source models, 2D and 3D smoothed seismicity models, fault-based and geodesy-based deformation models, SRMs for Italy's main active volcanic areas, and dedicated models for intraslab subduction seismicity. The project will also explore SRMs based on non-declustered catalogues that explicitly incorporate aftershocks and foreshocks.

For ground-motion modeling, the ISHM will select a wide range of GMMs suitable for shallow crustal, volcanic, and subduction environments. Selection criteria include data coverage and suitability for Italian seismotectonic contexts. The performance of the pre-selected GMMs will be tested against accelerometric datasets, to explore the predictive performance of models for seismic hazard purposes. A hybrid backbone approach will be evaluated for the explicit treatment of epistemic uncertainty.

Hazard calculations will be performed using the OpenQuake Engine platform (Pagani et al., 2014), supported by a dedicated computational infrastructure for reproducibility, version control, and data management. The ISHM will produce hazard curves and maps, uniform hazard spectra, disaggregation analyses, and related products for multiple ground-motion parameters and return periods.

A comprehensive testing phase will evaluate the reliability of the ISHM using available observations. To this purpose, both the SRMs and GMMs will be subjected to consistency evaluations, respectively comparing model outputs with past earthquakes (Schorlemmer et al., 2018) and accelerometric recordings (Scherbaum et al., 2009). These evaluations, based on statistical tests and model-performance metrics, will also guide logic-tree weighting, and ensure a scientifically robust integration of model components. Consistency checks will also be performed by comparing ISHM outputs against accelerometric and long-term macroseismic data collected across a wide range of sites (see e.g., Meletti et al., 2021; D'Amico et al., 2024). Comparisons will then be performed between the ISHM outcomes and previous PSHA models available for Italy (MPS04 and MPS19) and Europe (ESHM20, Danciu et al., 2021; 2024).

At the end of the project, the ISHM, together with its metadata and hazard products, will be made publicly accessible in accordance with INGV data policies.

References

D'Amico, V., Visini, F., Rovida, A., Marzocchi, W., and Meletti, C. (2024). Scoring and ranking probabilistic seismic hazard models: an application based on macroseismic intensity data, Nat. Hazards Earth Syst. Sci., vol. 24, 1401–1413, doi.org/10.5194/nhess-24-1401-2024.

Danciu, L., Giardini, D., Weatherill, G., Basili, R., Nandan, S., Rovida, A., et al. (2024). The 2020 European Seismic Hazard Model: overview and results. Nat. Hazards Earth Syst. Sci. 24, 3049–3073. doi: 10.5194/nhess-24-3049-2024

Danciu, L., Nandan, S., Reyes, C., Basili, R., Weatherill, G., Beauval, C., Rovida, A., Vilanova, S., Sesetyan, K., Bard, P.-Y., Cotton, F.,Wiemer, S., and Giardini, D. (2021). The 2020 update of the European Seismic Hazard Model: Model Overview, EFEHR Technical Report 001, v1.0.0, https://doi.org/10.12686/a15.

Meletti, C., Marzocchi, W., D'Amico, V., Lanzano, G., Luzi, L., Martinelli, F., Pace, B., Rovida, A., Taroni, M., Visini, F., and Group, M. W. (2021). The new Italian seismic hazard model (MPS19), Ann. Geophys., 64, SE112–SE112, https://doi.org/10.4401/ag-8579

Pagani, M, Monelli, D., Weatherill, G., Danciu, L., Crowley, H., Silva, V., Henshaw, P., Butler, L., Nastasi, M., Panzeri, L., Simionato, M., and Vigano, D. (2014). OpenQuake Engine: An Open Hazard (and Risk) Software for the Global Earthquake Model. Seismol. Res. Lett., 85(3), 692-702. https://doi.org/10.1785/0220130087.

Scherbaum, F., Delavaud, E., Riggelsen, C. (2009). Model selection in seismic hazard analysis: an information–theoretic perspective. Bull. Seismol. Soc. Am., 99(6):3234–3247.

Schorlemmer, D., Werner, M. J., Marzocchi, W., Jordan, T. H., Ogata, Y., Jackson, D. D., and Zhuang, J. (2018). The collaboratory for the study of earthquake predictability: Achievements and priorities. Seismol. Res. Lett., 89(4), 1305-1313.

Stucchi M., Meletti C., Montaldo V., Akinci A., Faccioli E., Gasperini P., Malagnini L., Valensise G. (2004). Pericolosità sismica di riferimento per il territorio nazionale MPS04. Istituto Nazionale di Geofisica e Vulcanologia (INGV). https://doi.org/10.13127/sh/mps04/ag

Tsunami inundation scenarios related to faults near the Italian Central Adriatic coast

C. Angeli[1], A. Armigliato[1], M. Zanetti[1], F. Zaniboni[1], S. Carcano[2,3], M. Forzese[2,4], L. Lipparini[2], I. Molinari[5]

[1] Alma Mater Studiorum – Università di Bologna, Dipartimento di Fisica e Astronomia "Augusto Righi", Bologna, Italy
[2] Istituto Nazionale di Geofisica e Vulcanologia, Sezione di Roma1
[3] Università degli Studi Roma Tre
[4] Università degli Studi di Catania
[5] Istituto Nazionale di Geofisica e Vulcanologia, Sezione di Bologna

The interaction of offshore activities with potential natural hazard sources is a critical issue for many energy and industrial applications. In recent years, growing attention has been devoted to tectonic and gravitative tsunami sources [1]. The present work was developed within the framework of the SPIN project ("Test delle Buone Pratiche per lo studio della potenziale interazione tra attività offshore e pericolosità naturali", in English "Test of good practices for the study of potential interaction between offshore activities and natural hazards") funded by the Italian Ministry of Environment and Energy Security (MASE). The project was a multidisciplinary collaboration among research institutes, Universities and Public Administrations and was completed in October 2025.

It followed previous projects on the study of (potentially) triggerable offshore seismicity, taking into account both the direct effects of induced earthquakes and the associated cascading effects, including triggered landslides and tsunamis generated either by the seismic event (seafloor deformation or faulting) or by coseismic gravitative failures. The ultimate goal of SPIN was to outline a methodology that strikes the right balance between national-scale survey and highly detailed analysis, such that it could potentially be applied as a routine procedure. The project focused on two study areas: "Alto Adriatico" (Northern Adriatic Sea), including the coasts of northern Marche and southern Emilia-Romagna and "Canale di Sicilia" (Sicily Strait), covering a portion of the southern coast of Sicily centred around the Gulf of Gela.

In this work, we present the workflow developed in the SPIN framework and used to model tsunamis generated by faults. In particular, applications to the "Alto Adriatico" study area are shown.

The first step of the proposed methodology consists of gathering geological and geophysical data for the target regions. These include multichannel 2D and high-resolution 3D seismic data, morpho-bathymetric data, instrumental seismicity records, and well data, which are used to characterize both shallow and deep tectonic features, including active faults. Once the geometry of

the considered fault is defined, the tsunami generation is modelled as an initial condition problem, where the initial deformation is determined by the coseismic displacement of the seafloor generated by the rupture of each fault. While a magnitude for each fault can be derived from its geometry using scaling laws [2], different distributions of slip on the fault are considered. In particular, we consider the case of uniform slip distribution, where the average slip is computed using Hanks-Kanamori formula [3], and cases of distributed slip, following the approach presented by [4]. After having computed the initial conditions, each scenario is simulated using the JAGURS software [5] to solve the Navier-Stokes equation in the Shallow Water approximation. The simulations are carried out on a system of nested grids, allowing for better spatial resolution in areas of interest, such as harbours and industrial complexes.

In the “Alto Adriatico” study area, five faults have been identified: four related to the Pesaro Thrust seismogenic structure and one, named Cornelia Thrust, located further south. For each fault, four scenarios have been considered, one with uniform slip and three with Gaussian slip distributions.

Particular attention has been given to strategic areas, where finer computational grids have been used. Such areas are the harbours in the cities of Pesaro, Fano, Senigallia and Ancona, and the Ancona Refinery.

In general, maximum observed inundation exceeds 1 m in most simulations in touristic beaches close to the source areas, as well as in coastal stretched hosting critical infrastructure, such as train tracks. The general pattern in maximum amplitudes is quite consistent among the different simulations. Special consideration is given to the interaction between incident tsunami waves and coastal structure such as river mouths and harbour structures, in order to determine possible amplification phenomena that may occur in such structures. This work represents a contribution towards a detailed hazard assessment at the local scale for the Italian Central Adriatic coastline.

References

[1] Antoncecchi I., Ciccone F., Dialuce G., Grandi S., Terlizzese F., Di Bucci D., Dolce M., Argnani A., Mercorella A., Pellegrini C., Rovere M., Armigliato A., Pagnoni, G., Paparo M.A., Tinti, S., Zaniboni F., Basili R., Cavallaro D., Coltelli M., Firetto Carlino M., Lipparini L., Lorito S., Maesano F.E., Romano F., Scarfì L., Tiberti M.M., Volpe M., Fedorik J., Toscani G., Borzi B., Faravelli M., Bozzoni F., Pascale V., Quaroni D., Germagnoli F., Belliazzi S., Del Zoppo M., Di Ludovico M., Lignola G.P., Prota A.; 2020: Progetto SPOT - Sismicità Potenzialmente innescabile Offshore e Tsunami. Report integrato di fine progetto. 44 p. DOI: 10.5281/zenodo.3732887 - ISBN: 9788894366945

[2] Leonard, M.; 2010: Earthquake fault scaling: Self-consistent relating of rupture length, width, average displacement, and moment release. Bulletin of the Seismological Society of America, 100(5A), pp.1971-1988.

[3] Hanks, T.C. and Kanamori, H.; 1979: A moment magnitude scale. Journal of Geophysical Research: Solid Earth, 84(B5), pp.2348-2350.

[4] Baglione E., Armigliato A., Pagnoni G., Tinti S.; 2018: Can simple magnitude-dependent 2D Gaussian representations of co-seismic slip distributions improve real time tsunami simulations? Geophysical Research Abstracts, 20, EGU2018-7096.

[5] Baba T., Takahashi N., Kaneda Y., Ando K., Matsuoka D., Kato T.; 2015: Parallel implementation of dispersive tsunami wave modeling with a nesting algorithm for the 2011 Tohoku tsunami. Pure appl. Geophys., doi:10.1007/s00024-015-1049-2, 2015.

Corresponding author: cesare.angeli2@unibo.it

To what extent b-positive is insensitive to catalogue incompleteness

Emanuele Biondini[1], Paolo Gasperini[2], Danijel Schorlemmer[3] , Laura Gulia[1,3]

[1] Dipartimento di Scienze della Terra, Università di Pisa, Pisa, Italy.
[2] Dipartimento di Fisica e Astronomia, Università di Bologna, Bologna, Italy.
[3] Swiss Seismological Service (SED), ETH Zurich, Zurich, Switzerland.

A new method to estimate the Gutenberg–Richter b-value, known as b-positive, was introduced by van der Elst (2021) as a robust estimator designed to mitigate the effects of transient catalogue incompleteness that commonly bias b-value computations, particularly during periods of intense aftershock activity. Despite its growing use, a systematic and quantitative assessment of its sensitivity to the magnitude of completeness under realistic detection conditions is still lacking.

Here we evaluate the robustness of b-positive to catalogue incompleteness using large ensembles of synthetic earthquake catalogues generated with the ETAS model. The simulations reproduce both background-driven seismicity and aftershock-dominated sequences initiated by large mainshocks and explicitly account for short-term aftershock incompleteness through time-dependent detection thresholds. By systematically varying the assumed completeness magnitude, we quantify the bias and variability of b-positive estimates under controlled but realistic conditions.

The same analysis is performed for other available b-value estimation techniques, including b-more positive and b-more incomplete (Lippiello & Petrillo, 2024), allowing a direct comparison of estimator performance across different seismicity regimes and levels of catalogue incompleteness. Results show that b-positive and b-more positive substantially reduce the systematic underestimation of b-values observed for classical magnitude-based approaches in incomplete and strongly clustered catalogues, while maintaining stable behaviour over a wide range of completeness conditions. These findings provide quantitative support for the use of difference-based b-value estimators in automated and near-real-time seismicity monitoring frameworks, such as the updated Foreshock Traffic Light System (Gulia & Wiemer, 2019; Gulia et al., 2024).

References

Gulia, L., and S. Wiemer; 2019: Real-time discrimination of earthquake foreshocks and aftershocks, Nature Vol. 574, pp. 193–199, https://doi.org/10.1038/s41586-019-1606-4.

Gulia, L., S. Wiemer, E. Biondini, B. Enescu and G. Vannucci; 2024: Improving the Foreshock Traffic Light Systems for real-time discrimination between foreshocks and aftershocks, SRL, Vol. 95 (6): pp. 3579–3592, https://doi.org/10.1785/0220240163.

Lippiello, E. & Petrillo, G.; 2024: b -More-Incomplete and b -More-Positive: Insights on a Robust Estimator of Magnitude Distribution. J. Geophys. Res. Solid Earth, 129, e2023JB027849, https://doi.org/10.1029/2023JB027849

van der Elst, N. J.; 2021. B-positive: A robust estimator of aftershock magnitude distribution in transiently incomplete catalogs, J. Geophys. Res. 126, e2020JB021027, https://doi.org/10.1029/2020JB021027.

Corresponding author: emanuele.biondini@dst.unipi.it

Data-Driven Empirical Modeling of Source Directivity Effects in a Ground Motion Model for Central Italy

L. Colavitti[1], G. Lanzano[2], S. Sgobba[2], F. Pacor[2]

[1] *University of Genoa, Department of Earth, Environmental and Life Sciences, Genoa, Italy*
[2] *Istituto Nazionale di Geofisica e Vulcanologia – INGV, Milan, Italy*

Assessing the spatial variability of seismic shaking in the epicentral area of an earthquake is one of the major challenges to be addressed in seismic hazard estimates. Among the main contributions to the ground motion variability, the source directivity plays a predominant role, inducing spectral amplifications in the direction of rupture propagation, even for small to moderate magnitude earthquakes.

In this work, we present a fully data-driven approach to parameterize rupture directivity effects within a non-ergodic Ground Motion Model (GMM) for Central Italy. The model is developed using a dataset of 456 normal-fault earthquakes (M_W 3.2–6.5) recorded between 2009 and 2018.

Following the same approach as described in Colavitti et al. (2022), source directivity is isolated as part of the aleatory residual component after systematically removing source, path, and site contributions through GMM calibration. The analysis is performed in terms of acceleration response spectra (SA), with the explicit goal of improving seismic hazard applications. We observed that approximately 30% of the analyzed events exhibit clear directivity signatures: directivity effects are more pronounced in SA, showing broader frequency bands and larger peak amplitudes compared to Fourier Amplitude Spectra (FAS).

The directivity correction model is based on three empirical relations which describe:

i) azimuthal variations modeled via a theoretical directivity factor C_d (Boatwright, 2007);

ii) spectral variation of directivity amplitude using a first-order Gaussian function;

iii) the correlation between M_W and the period of maximum directivity effect.

The validity of the method is extended to higher magnitudes using pulse-like periods T_p of global normal faulting earthquakes, included in the NESS2 database (Sgobba et al., 2021).

A key result is the empirical scaling between Mw and the period of maximum directivity, suggesting that directivity effects scale continuously from small to large earthquakes, shifting toward higher frequencies for weaker events. Model predictions indicate azimuth-dependent spectral amplifications of up to a factor of three relative to non-directive cases. Incorporating the directivity correction into the non-ergodic GMM leads to a significant reduction of aleatory variability, with standard deviation decreases of 13–20% across the analyzed periods. These results demonstrate the robustness and scalability of the proposed directivity parametrization and highlight its potential for generating realistic shaking scenarios and improving seismic hazard assessments.

Future developments will focus on extending the dataset (e.g. ITACAext 2.0: Lanzano et al. 2025), period range, fault geometrical representation, and the probabilistic treatment of directivity parameters for full integration into PSHA frameworks.

References

Boatwright, J.; 2007: The persistence of directivity in small earthquakes. Bulletin Seismological Society of America 97, 1850–1861. https://doi.org/10.1785/0120050228.

Colavitti, L., Lanzano, G., Sgobba, S., Pacor, F. and Gallovič, F; 2022: Empirical evidence of frequency-dependent directivity effects from small-to-moderate normal fault earthquakes in Central Italy. Journal Geophysical Research - Solid Earth 127, e2021JB023498. https://doi.org/10.1029/2021JB023498.

Lanzano, G., Vitrano, L., Bindi, D., Felicetta, C., Sgobba, S., Luzi, L. and Pacor, F.; 2025: ITACAext2.0: A High-Quality Parametric Table of Strong-to-Weak Motion Recordings for Seismological and Engineering Research in Italy. Seismological Research Letters 96(5): 3295-3316. https://doi.org/10.1785/0220240309.

Sgobba, S., Felicetta, C., Lanzano, G., Ramadan, F., D'Amico, M. and Pacor, F.; 2021: NESS2.0: An Updated Version of the Worldwide Dataset for Calibrating and Adjusting Ground-Motion Models in Near Source. Bulletin Seismological Society of America **111**, 5, 2358–2378, https://doi.org/10.1785/0120210080.

Corresponding author: leonardo.colavitti@edu.unige.it

First Deployment of Tsunami Buoys in the Central Mediterranean Sea: System Description, Installation, and Operational Overview

A. Costanza[1], F. Macaluso[2], A. Di Benedetto[2], F. Romano[2], S. Lorito[2], A. Amato[2], G. Marinaro[3], H.B. Bayraktar[2], S. Bruni[2], G. Selvaggi[2], A. Piatanesi[2], M. Volpe[2], N. Kalligeris[4]

[1] *Istituto Nazionale di Geofisica e Vulcanologia (INGV), Sezione Osservatorio Etneo*
[2] *Istituto Nazionale di Geofisica e Vulcanologia (INGV), Sezione Osservatorio Nazionale Terremoti*
[3] *Istituto Nazionale di Geofisica e Vulcanologia (INGV), Sezione Roma2*
[4] *Institute of Geodynamics, National Observatory of Athens (NOA), Athens, Greece*

For the first time in the Mediterranean Sea, two tsunami buoys (Tsunami Buoy INGV 01 and 02) have been successfully deployed in the Ionian Sea (Fig. 1), as part of the Italian Tsunami Alert Centre (CAT-INGV), which operates within the National Alert System for Tsunamis generated by earthquakes in the Mediterranean Sea (SiAM), composed also by National Civil Protection Department and Italian Institute for Environmental Protection and Research. CAT-INGV is also a Tsunami Service Provider in the NEAMTWS (North Eastern Atlantic, Mediterranean and connected seas Tsunami Warning System), coordinated by Intergovernmental Oceanographic Commission of UNESCO (IOC-UNESCO), along with CENALT (Centre d'alerte aux tsunamis, France), NOA (National Observatory of Athens, Greece), KOERI (Kandilli Observatory and Earthquake Research Institute, Türkiye) and IPMA (Instituto Português do Mar e da Atmosfera, Portugal). The buoys have been developed by the Mediterraneo Senales Maritimas company (MSM, Spain) in collaboration with the Istituto Nazionale di Geofisica e Vulcanologia (INGV, Italy) in the framework of MEET (https://meet.ingv.it/), a project coordinated by INGV and funded by the European Union through the National Recovery and Resilience Plan. Real-time sea level monitoring and rapid tsunami detection in the open ocean are critical for assessing tsunami wave propagation and the potential impact on coastal areas. The deployment of these buoys represents a major advancement in tsunami preparedness in the Mediterranean Sea. Unfortunately, one of the mooring of one buoy (Tsunami Buoy INGV 02) recently broke, because it was likely unintentionally damaged, but thanks to the tracking system, the buoy could be recovered. The re-deployment is presently being planned for 2026.

The tsunami buoy system is composed of three primary components: the surface buoy (EBM24-TS), two ocean Bottom Pressure Recorders (BPRs), and a web-based Control Center for data acquisition, monitoring, and alert generation. The buoys were deployed at the following coordinates: Tsunami

Buoy INGV 01 at 36°49'48.00''N – 16°30'00.00''E (Ionian Sea, ~100 km offshore of Siracusa, eastern Sicily, at a depth of ~3200 m) on 14 September 2025, and Tsunami Buoy INGV 02 at 38°39'36.00''N – 18°09'36.00''E (~100 km offshore of Crotone, eastern Calabria, at a depth of ~2600 m) on 16 September 2025. The deployment points are shown in Fig. 1. These points were chosen with an optimisation procedure aimed at minimizing the detection time of any tsunami, with weights based on the tsunami source probability (Basili et al., 2021; Romano et al., 2024). The vessel employed for deployment, Christos LVII, was equipped with a telescopic crane capable of lifting the 4-ton sinker, auxiliary boat for towing, diver support, and full power and communication infrastructure for telemetry and testing. Each buoy communicates acoustically with one BPR at a time and transmits near-real-time data via satellite to the CAT-INGV; a second BPR is available as a redundant unit and can be remotely activated in case of malfunction of the primary BPR.

The EBM24-TS buoy is specifically designed for deep-sea deployment up to 7,000 m and is compliant with IALA (International Association of Marine Aids to Navigation and Lighthouse Authorities) recommendations for visibility, safety, and navigational aids (AtoN). It features a high-buoyancy polyethylene-foam elastomer-coated float (>3,100 kg), an aluminum marine superstructure housing electronic modules in IP66 enclosures, solar panels with redundant batteries ensuring over ten days of autonomy, a 360° LED marine lantern with 8 NM visibility, a radar reflector with Radar Cross Section (RCS)>10 m^2, Automatic Identification System (AIS) Type 1 transmitter, and antivandalism systems including GPS positioning, intrusion sensors, and impact alarms. The tail includes sacrificial anodes, adjustable steel ballast, and a support for the Surface Modem Transceiver (SMT) acoustic transducer.

The CPU on board the buoy is a 32-bit high-performance unit with a real-time operating system, low-power design, remote configurability, 32 GB storage, and compatibility with serial and analog sensor interfaces. It supports satellite communications via dual Iridium SBD (Short Burst Data) modems, enabling both periodic telemetry transmission and immediate event-driven alerts. The SMT acoustic transceiver operates at 14–19 kHz, featuring bidirectional telemetry to ensure robust communication with the BPR.

The BPR is a compact, high-capacity unit with acoustic release, digital signal processing, lithium battery with a theoretical deployment of over 1,450 days, a quartz pressure sensor, and the capability to detect pressure variations of 3 cm (configurable remotely) to trigger immediate data transmission to the buoy. The BPR includes a tilt sensor and a suspension float ensuring verticality during deployment. Its anchoring system is hydrodynamically optimized for minimal drift and controlled descent, with acoustic release enabling recovery.

The general layout of the mooring and data transmission system is shown in Fig. 2.

The deployment operations were carefully planned and executed in sequential phases:

- Phase A: Deployment of buoy and rope system, including intermediate floats.
- Phase B: Anchoring of the sinker and stabilization of the buoy.
- Phase C: Underwater inspection of the buoy and anchor chain by professional divers.
- Phase D: Deployment and commissioning of the BPRs, with acoustic testing and monitoring.
- Phase E: Remote operational testing, verification of communication and system functionality via the Tsunami Sentinel web software.

Some of these phases are shown in Fig. 3.

The Control Center leverages the Tsunami Netcom TS web application, enabling remote monitoring and management of buoy and BPR networks, near real-time visualization of pressure data, operational status of electronic subsystems, and alarm management, including battery, position, intrusion, impact, and communication faults. Netcom TS supports remote command issuance, system reconfiguration, event simulation, integration with the NOAA NDBC (National Oceanic and Atmospheric Administration - National Data Buoy Center) network (https://www.ndbc.noaa.gov/), and comprehensive maintenance and statistical logging for all deployed units.

The deployment of these buoys establishes a robust infrastructure for continuous monitoring of the seafloor pressure, providing critical data to improve tsunami detection, modelling, and early warning capability.

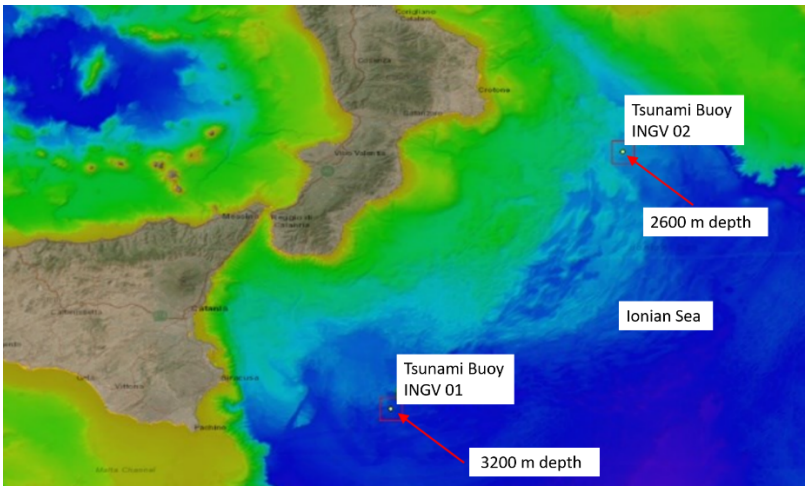

Fig. 1 – Deployment locations of the two buoys

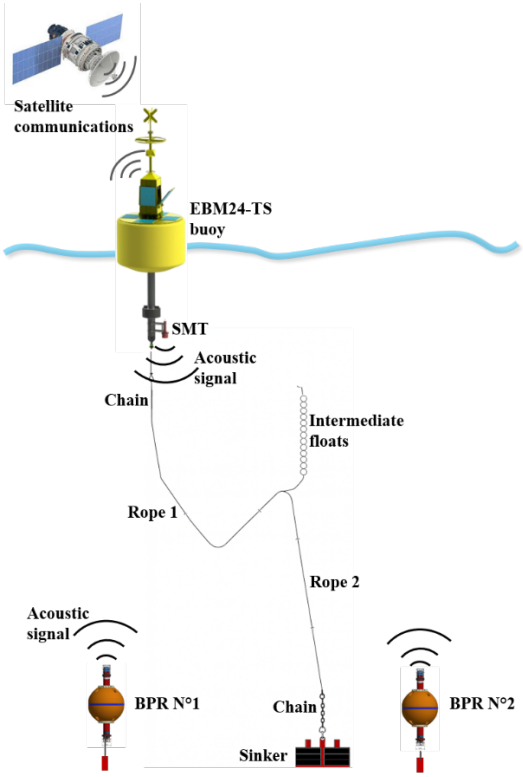

Fig. 2 – General layout of the mooring and data transmission system.

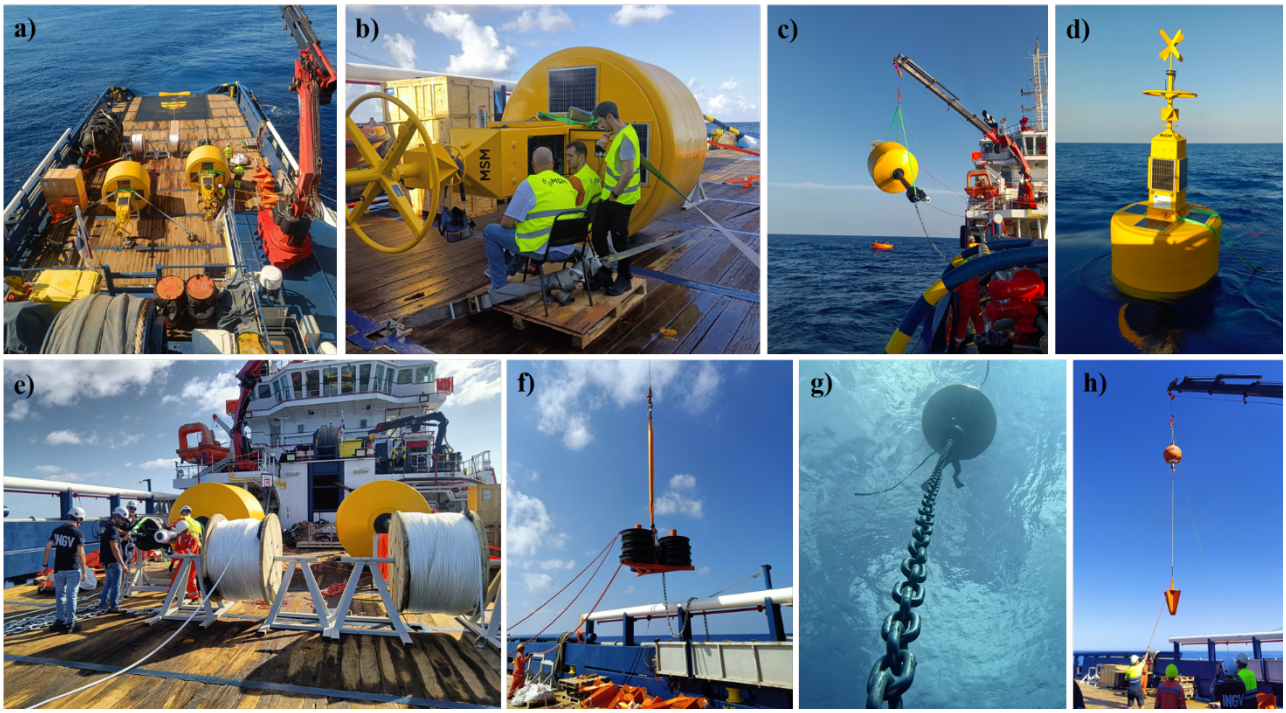

Fig. 3 – a) Tsunami Buoys during transit to the deployment sites; b) Configuration and testing of the buoys on board the vessel; c) During the buoy deployment phase; d) Buoy just positioned in the sea, but not yet anchored; e) Paying out the mooring lines for anchoring the buoy to the sinker; f) During the deployment of the sinker; g) Underwater inspection of the buoy and anchor chain; h) During the deployment of the BPR sensor.

References

Basili, R., Brizuela, B., Herrero, A., Iqbal, S., Lorito, S., Maesano, F.E., Murphy, S., Perfetti, P., Romano, F., Scala, A., Selva, J., Taroni, M., Tiberti, M.M., Thio, H.K., Tonini, R., Volpe, M., Glimsdal, S., Harbitz, C.B., Løvholt, F., Baptista, M.A., Carrilho, F., Matias, L.M., Omira, R., Babeyko, A., Hoechner, A., Gürbüz, M., Pekcan, O., Yalçıner, A., Canals, M., Lastras, G., Agalos, A., Papadopoulos, G., Triantafyllou, I., Benchekroun, S., Agrebi, Jaouadi, H., Ben, Abdallah, S., Bouallegue, A., Hamdi, H., Oueslati, F., Amato, A., Armigliato, A., Behrens, J., Davies, G., Di, Bucci, D., Dolce, M., Geist, E., Gonzalez, Vida, J.M., González, M., Macías, Sánchez, J., Meletti, C., Ozer, Sozdinler, C., Pagani, M., Parsons, T., Polet, J., Power, W., Sørensen, M., Zaytsev, A.; 2021: The Making of the NEAM Tsunami Hazard Model 2018 (NEAMTHM18). Front. Earth Sci. 8:616594. doi: 10.3389/feart.2020.616594

Romano, F., Lorito, S., Piatanesi, A., Volpe, M., Bayraktar, H. B., Kalligeris, N., Amato, A.; 2024: Optimal positioning of two deep ocean bottom pressure gauges for tsunami wave detection in the western Ionian Sea, EGU General Assembly 2024, Vienna, Austria, 14–19 Apr 2024, EGU24-18892, https://doi.org/10.5194/egusphere-egu24-18892

Corresponding author: antonio.costanza@ingv.it

Towards a Unified PFDHA Platform: OpenQuake Engine Implementation

Hugo Fernandez[1-2], Yen-Shin Chen[1-3], Marco Pagani[3], Laura Peruzza[1]

[1] *Istituto Nazionale di Oceanografia e di Geofisica Sperimentale–OGS Centro di Ricerche Sismologiche, Trieste, Italy*
[2] *Università degli Studi "G. D'Annunzio", Chieti-Pescara, Italy*
[3] *GEM Foundation, Pavia, Italy*

In the frame of ended and ongoing projects (Boncio et al., 2025; Caputo et al., 2025; https://sigma-programs.com/), we will present the workflow that has been implemented to compute Probabilistic Fault Displacement Hazard Assessment (PFDHA) compliant with the OpenQuake Engine (Pagani et al., 2014; Chen et al., 2025), and a first, trial, application to Southern Italy (Northern Calabria).

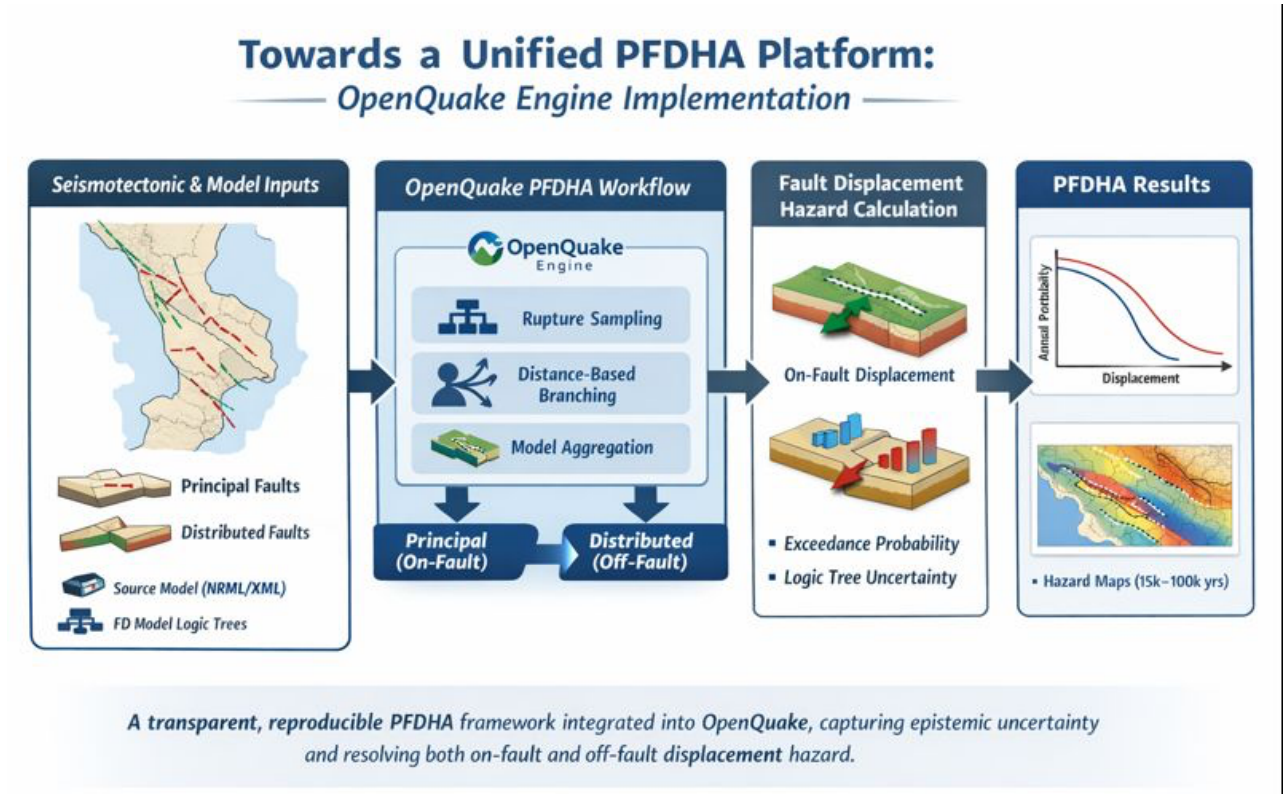

Fig. 1 – Graphical abstract of the work.

We demonstrated the workflow capability through end-to-end calculations covering both on-fault (principal) and off-fault (distributed) displacement scenarios.

The Calabria case study highlights the importance of logic tree approaches to capture epistemic uncertainties arising from different model formulations, parameter selections, and source configurations.

Acknowledgments

Research funds for the PhD grant of H. Fernandez derive from NextGeneration EU Mission 4 Component 2 PNRR Project GEOSCIENCES IR (ISPRA coord.) IR000037 – CUPI53C22000800006 – OGS03 Research Unit on WP4 - Activity 4.3 Active and capable faults.

References

Boncio, P., Peruzza, L., Pace, B., Testa, A., Fernandez, H., Chen, Y.S.; 2025: *Valutazione della pericolosità sismica da fagliazione superficiale della Diga Farneto del Principe in Comune di Roggiano Gravina (CS) - Relazione della FASE 3*. Convenzione CUP B47I18075860006, INGEO-OGS, Rapporto interno OGS-2025/113, https://hdl.handle.net/20.500.14083/46003, Chieti-Trieste, 75 pp.

Caputo, R., Peruzza, L., Seno, S., Tibaldi, A., and Falcucci, E.; 2025: *Fault segmentation and seismotectonics of active thrust systems: the Northern Apennines and Southern Alps laboratories for new Seismic Hazard Assessments in northern Italy (NASA4SHA)*. Misc. INGV, 102: 1-152, https://doi.org/10.13127/misc/102

Chen, Y.S., Pagani, M., Fernandez, H., and Peruzza, L.; 2025: *Prototypal Implementation of Probabilistic Fault Displacement Hazard Assessment Using the OpenQuake Engine Components*. 43 Convegno GNGTS, Atti, Bologna. https://hdl.handle.net/20.500.14083/43865

Pagani, M., Monelli, D., Weatherill, G., Danciu, L., Crowley, H., Silva, V., Henshaw, P., Butler, L., Nastasi, M., Panzeri, L., Simionato, M., and Vigano, D.; 2014: *OpenQuake Engine: An open hazard (and risk) software for the Global Earthquake Model.* Seismological Research Letters, 85 (3), 692-702. https://doi.org/10.1785/0220130087

Corresponding author: hfernandez@ogs.it

Scientific contributions from twenty years of CIEN recordings

C. Fidani[1]

[1] *Central Italy Electromagnetic Network, San Procolo, Fermo, Italy*

The Central Italy Electromagnetic Network (CIEN) was established on January 1, 2006, with the activation of its first monitoring station in the Marche countryside in the province of Fermo, central Italy. As a non-profit organisation, its main goal is to characterise any electromagnetic phenomena that may occur during earthquakes. The objective emerged from an investigation carried out over the previous eight years, first addressing the macroscopic phenomena observed during past earthquakes in central Italy and then reading studies already concluded or underway in various countries. The investigation led to the publication of a book in Italian (Fidani, 2005) and an international report (Fidani, 2006), which described the activity carried out. Furthermore, a period of electronic experimentation took place over the previous four years, simultaneously with the collection of numerous publications and the writing of the book, based on the experiments carried out by various authors. The spark that inspired this project dates back to the summer of 1987, when a long-wave radio receiver highlighted strong reception disturbances noted in an electronic construction diary, and a moderate intensity earthquake struck Porto San Giorgio in the Marche region a few days later (Battimelli et al., 2019). The consolidation of that inspiration came unexpectedly with the reading of an article dedicated to the construction of a radio listening receiver in November of the same year, whose lines apparently described the sounds heard months before (Cerboni and Veronese, 1987).

Starting in 2008, additional stations joined the network, reaching 14 in 2015; subsequently, the number decreased to three currently operational stations: those of Fermo, Perugia, and Gubbio. The stations were equipped with the same instrument for recording the electrical component in at least two horizontal directions. Recordings were limited to time-varying signals in the ELF bands between 4 Hz and 1 kHz and VLF bands between 1 kHz and 20, 50, or 100 kHz, depending on the sound card used. As monitoring progressed, additional instruments were added over time and at different stations, depending on availability, site characteristics, and the checks suggested during attempts to understand the signals. The duration and type of monitoring activities carried out during the life of CIEN are represented by the horizontal extensions of the bars in Figure 1. Specifically, vertical electrical conductivity sensors, magnetometers operating in the same ELF band, alpha, beta, and gamma particle detectors, ion counters, microphones, weather stations, thermometers, hygrometers, GPS, and CO_2 sensors have been added; the sensor type is reported by the colour of

the bars relative to each station in Figure 1. CIEN recorded atmospheric electrical signals in the ELF band during the three main Italian seismic swarms that occurred after the Umbria-Marche earthquake: the 2009 L'Aquila, 2012 Modena, and 2016-2017 Amatrice-Norcia-Montareale earthquakes, while monitoring the VLF and LF bands during the latter two seismic swarms.

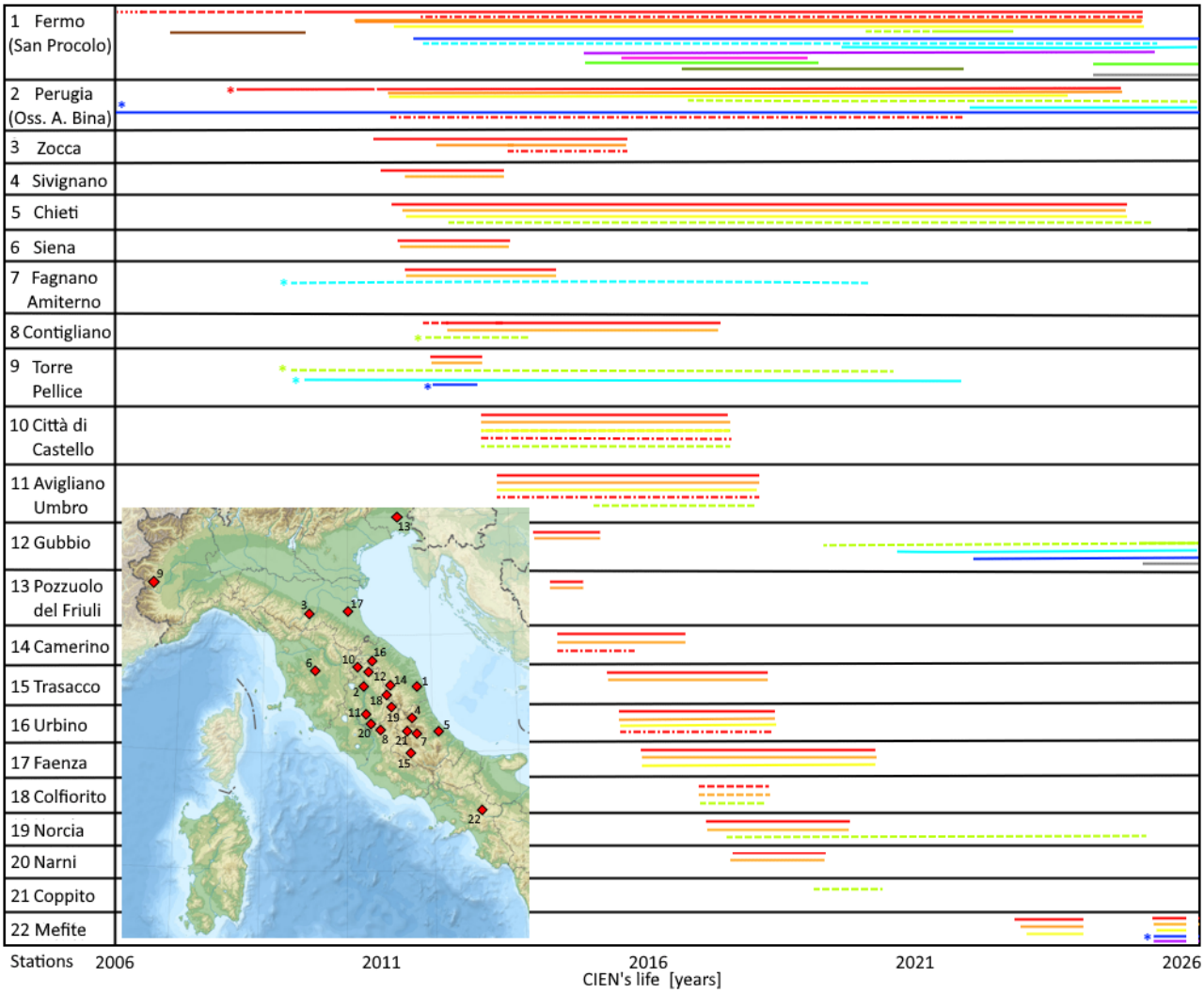

Fig. 1 – CIEN stations during the network activity, where colours indicate the type of instruments. Dotted red: ELF recorded 12/24h in one direction; dashed red: ELF in one direction; dashed dotted red: z direction; continuous red: ELF in two directions; orange: VLF; yellow: LF; dashed green: magnetic in one direction; Brown: OL radio; continuous green: magnetic in two directions; night blue: meteo station; violet: ground thermometer; pink: ion counter; dashed sky blue: gamma counter; continuous sky blue: Radon; black green: GPS; grey: CO_2. The red * indicates the north Perugia station; the other *s indicate instruments not CIEN. The locations of the stations are shown on a map.

Monitoring the atmospheric electric field component in the ELF band, between 4 Hz and 1 kHz, over such a long period is a global first for this type of monitoring. CIEN's scientific contributions can be summarised in five categories: the construction of sensors for long-term acquisition, the creation of suitable databases, the development of data analysis methods, the hypothesis of some models to interpret observations, and the disclosure of observations with obtained results. Sensor buildings developed three slightly different electronics with improved performance to amplify induced

atmospheric electric signals, while the sensor and acquisition hardware were always the same: a horizontal wire and the sound card of a PC. Although uninterruptible power supplies (UPS) ensured the acquisitions continued to operate during brief power outages, a significant portion of the time was spent on network maintenance. Indeed, the sensors' exposure to adverse weather conditions required numerous recording restoration operations, including some system replacements, to reduce data gaps.

The first electronics consisted of a simple audio amplifier realised by two integrated circuits, one operational amplifier and one power amplifier. The second electronics was a much simpler audio amplifier made by one integrated circuit, realising an integrator. The third electronics maintained the simplicity of the second project, improving sensitivity and enlarging the frequency band. A variant of the electronics using a flat sensor was supported by Father Martino Siciliani as the subject of a new project to be developed at the "A. Bina" Seismic Observatory in Perugia. The Umbria Region funded the project for the development of a patent for an electrodynamic rain gauge, represented in Figure 2. Indeed, the Benedictine Monastery in Perugia, directed by Father Martino until 2025, was also a centre for meteorological studies in 1639, when Father Benedetto Castelli invented the first rain gauge together with Galileo Galilei. The invention was accepted on January 30, 2019, under No. 102016000077834. Moreover, the invention's capabilities were described in a recent publication (Fidani and Siciliani, 2025).

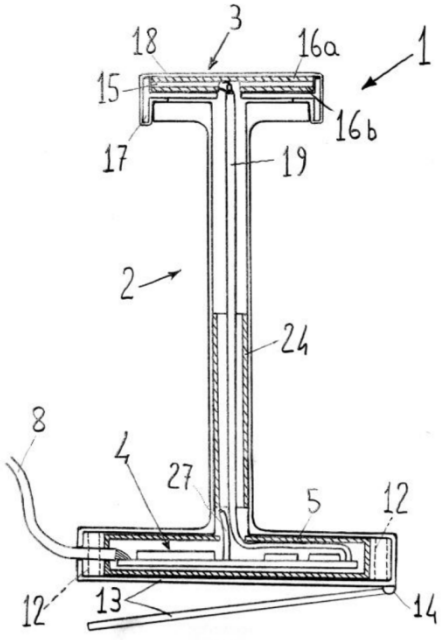

Fig. 2 – The electrodynamic pluviometer sketch with the numeration of its parts. See the patent N. 102016000077834 for further details regarding all parts and electronics. The pluviometer comprises an insulating housing (2), a capacity sensor (3) consisting in a capacitor having a first armature (16a) exposed to the raindrops to be sensitive to the variation in electric charge induced by said raindrops, and electrically shielded electronics (4) for conditioning of the signal generated by said capacity sensor (3) are positioned inside said insulating housing (2).

The composition of a database of atmospheric electrical recordings in ELF and VLF bands satisfied the necessity of recording the elements considered significant, for fast data consulting, and taking into account space memory limitations. Thus, spectrograms were the preferred solution, considering a logarithmic spectrum for the ELF band to highlight the lower frequencies, and a linear spectrum for the VLF band to distinguish the transmitting carriers. The other characteristics of the spectrograms have been described in publications from the outset (Fidani, 2011). The CIEN recording database, until 2014, with a few exceptions until 2016, consists of recordings with a sampling frequency of 2 kHz and 16-bit conversion, on the two channels corresponding to the pair of electrodes at each station arranged orthogonally. The database was supplemented by text files since 2012, which stored the intensities of the VLF stations, and subsequently, since 2016, by text files storing the intensities of the Schumann Resonances (Fidani and Marcelli, 2017).

Analysis methods were developed to characterise specific signals in the spectrum and statistically verify their possible relationships with earthquakes. The first method was implemented using software such as Spectrumlab and Audacity, which could sum and filter certain regions of the spectrum. This allowed for correcting the bandwidth of sound cards, subtracting noise or part of it from the signal, and isolating signals recorded during seismic events (Fidani, 2011). The second method was derived from the definition of digital event-to-event covariance (ELF) to calculate the probability of an earthquake occurring after an ELF observation. In this formulation, the conditional probability of recording an earthquake with a magnitude greater than M_0 after observing a given ELF intensity was derived from the correlation factor. The method enabled the identification of a significant peak of correlation between ELF observations that anticipate small earthquakes within 70 km by 6 days (Fidani and Marcelli, 2025) and defined the probability of an earthquake within a certain number of days from the observation, shown in Figure 3.

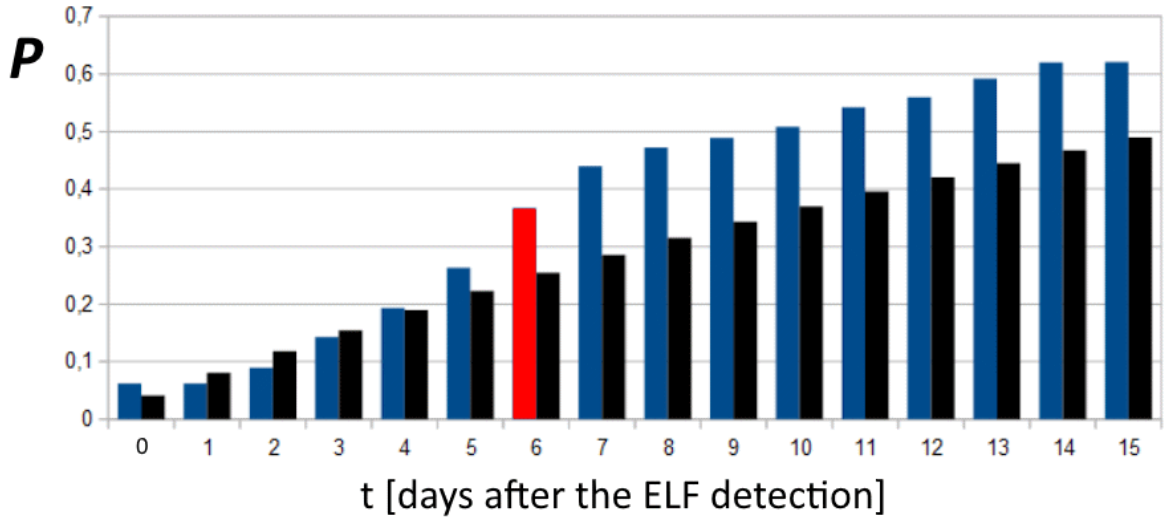

Fig. 3 – The probability of occurrence of an earthquake in the given time interval after an ELF observation, in blue, under the hypothesis of a generalised Poisson process. The probability without ELF detection is black. The probability step on the sixth day after the ELF detection, in red, corresponds to the significant correlation peak.

Various hypotheses have been formulated regarding the nature of CIEN's observations of atmospheric electric fields, magnetic fields, and gases. Regarding atmospheric electric field oscillations, clouds of electrified molecules, capable of remaining stable for a certain duration, have been proposed (Fidani and Martinelli, 2015). The model allowed us to estimate the amount of charge present in the clouds. These clouds should be expelled from the ground in the days preceding seismic events, thanks to the increased flow of fluids in the subsurface, probably driving the radon gas. Regarding magnetic pulses, impulsive telluric currents have been proposed (Fidani et al., 2020). The model allowed us to estimate the currents required to generate the magnetic measurements. These currents should be impulsively interrupted by sudden changes in conductivity in the hypocentral region in the days preceding strong earthquakes.

Dissemination has been achieved through seminars dedicated to recurring events, in secondary schools, universities, and associations; through presentations at national and international conferences; publications in proceedings and international peer-reviewed journals; and through several websites. Specifically, CIEN has been the subject of 14 seminars, primarily for dissemination purposes, and has been presented at 32 national and international conferences. One book has been published in Italian, 46 conference proceedings, and 5 international journal papers have been published. Finally, real-time recordings from some of the network's stations were published on the "A. Bina" Seismic Observatory website until 2015, while various information is now available on the network's webpage http://cfidani.wixsite.com/cien. The data were obtained from the CIEN and contain proprietary information. Access to these data is subject to ethical and legal restrictions and was granted to the authors under approval from the CIEN committee. The data are therefore not publicly available. However, qualified researchers may request access to the data by submitting a proposal to the corresponding author, subject to approval and the execution of a data-use agreement.

References

Battimelli E.; Adinolfi G. A.; Amoroso O.; Capuano P.; 2019: Seismic Activity in the Central Adriatic Offshore of Italy: A Review of the 1987 ML Porto San Giorgio Earthquake. Seismological Research Letters, 90 (5): 1889–1901.

Cerboni A.; Veronese F.; 1987: Alla scoperta delle VLF. Progetto elektor, 11, 75-81.

Fidani C.; 2005: Ipotesi sulle anomalie elettromagnetiche associate ai terremoti. First ed. Libreria Universitaria Benedetti L'Aquila, L'Aquila, Italy, 300pp.

Fidani C.; 2006: On Electromagnetic Precursors of Earthquakes: Models and Instruments. IPHW proceedings, Bologna, June 17, pp. 25-41.

Fidani, C.; 2011: The Central Italy Electromagnetic Network and the 2009 L'Aquila earthquake: observed electric activity. Geosciences, 1, 3-25.

Fidani, C.; Martinelli, G.; 2015: A possible explanation for electric perturbations recorded by the Italian CIEN stations before the 2012 Emilia earthquakes. Boll. Geofis. Teor. Appl. 56, 211–226.

Fidani, C.; Marcelli, D.; 2017: Ten Years of the Central Italy Electromagnetic Network (CIEN) Continuous Monitoring. Open Journal of Earthquake Research, 6, 73-88.

Fidani, C.; Orsini, M.; Iezzi, G.; Vicentini, N.; Stoppa, F.; 2020: Electric and Magnetic Recordings by Chieti CIEN Station During the Intense 2016–2017 Seismic Swarms in Central Italy. Front. Earth Sci. 8:536332.

Fidani, C.; Marcelli, D.; 2025: The statistical correlations between the electric oscillations detected by CIEN and moderate seismic activity, 43rd GNGTS session 2.1, Bologna, p. 39-43, February 11-14.

Fidani, C.; Siciliani, M.; 2025: Low-Cost Electrodynamic Pluviometers for Flood and Debris Flow Monitoring. Sustainability 2025, 17, 9662. https://doi.org/10.3390/su17219662

Corresponding author: c.fidani@virgilio.it

Ground Motion Prediction Equations for Calabria (Italy) based on regional earthquakes data (3.4 ≤ M ≤ 5.2)

D. Galluzzo[1], M. Ponte[2], M.G. Soldovieri[1], M. La Rocca[2]

[1] Istituto Nazionale di Geofisica e Vulcanologia, sez. Osservatorio Vesuviano, Napoli
[2] Università degli Studi della Calabria, Cosenza

Ground Motion Prediction Equations (GMPEs) for Calabria (Italy) have been developed using a dataset of 101 crustal earthquakes with magnitude ranging from 3.4 to 5.2, recorded between 2010 and 2025 by a dense seismic network of 109 stations. A GMPE is a mathematical model that estimates the expected level of ground shaking at a specific location, given certain earthquake parameters such as magnitude, distance from the source, and local site conditions. These equations allow scientists to predict the amplitude of ground motion in time and frequency domain for future seismic events. This work focuses on the estimation of a ground motion model (GMM) for Calabria through the analyses of earthquakes located in the Calabrian arc with the aim of obtaining a model as reliable as possible for the investigated area. Calabria is one of the regions with the highest seismic hazard in Italy because of its tectonic features and of its seismic history. We computed empirical attenuation models for peak ground velocity (PGV), peak ground acceleration (PGA), and 5%-damped spectral acceleration (SA) at selected periods. If IM indicates the intensity measure (PGV, PGA or SA), in this study, we assumed $\log_{10}$(IM) as a linear function of magnitude M and of $\log_{10}$(R) where R is the hypocentral or epicentral distance. The GMPEs were obtained through least-squares regression of ground motion parameters as a function of magnitude and distance.

Available seismic recordings of recent earthquakes were visually inspected to select only those characterized by high signal to noise ratio. Seismograms were deconvolved for the instrument response in order to deal with a uniform dataset. The total number of source-station paths used in our analysis is 4867. This large number associated with the spread distribution of epicenters and a fairly uniform seismic network ensures a very good coverage of the Calabria land.

Figures 1 shows the values of PGV (Fig. 5a), PGA (Fig. 5b), and SA ground motion models (5% of damping and T=1.0 s; Fig. 5c) and the peak values obtained from the signals of all the M4.0 earthquakes.

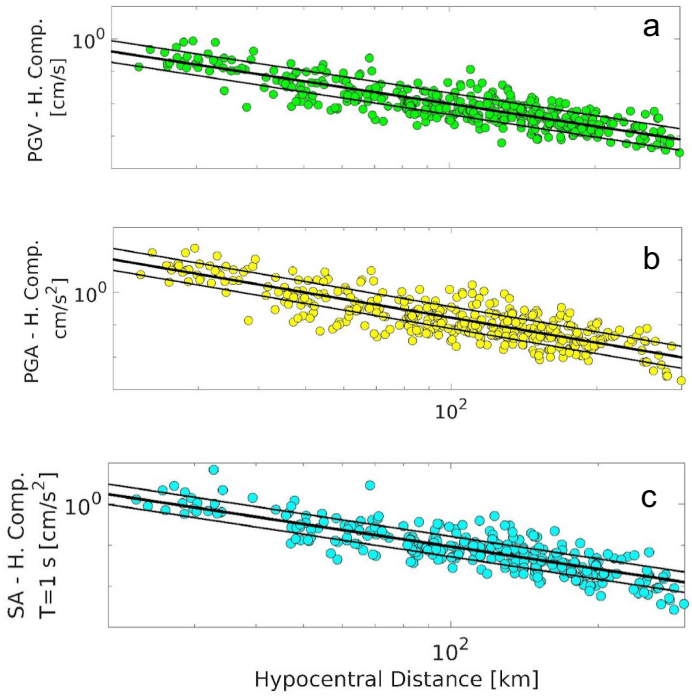

FIG.1. Ground motion models (black line) for PGV, PGA and SA (horizontal component) vs hypocentral distance for M4.0 and the observed peak amplitudes (PGV, PGA and SA are shown in green, yellow and blu circles respectively).

The model obtained in this work and the models of Bindi et al. (2011) (ITA10) and Lanzano et al. (2019) (ITA18) are within the calculated error. The comparison with established GMPEs ITA10 (Bindi et al., 2011), ITA18 (Lanzano et al., 2019) and D'Amico et al. (2018) (DAM18) shows a high similarity in the distance range 20 km – 90 km and slightly lower amplitude values for distance larger than about 100 km. The lower values at medium-to-large distance correspond to a slightly higher attenuation. These results support the use of specific regional ground motion models for more accurate seismic hazard assessments in Calabria and other tectonic contexts.

Results are very robust in the distance range from about 20 km to at least 250 km. Distances shorter than 20 km are very few in our dataset, and none is shorter than 10 km. It is well established that GMPEs are most reliable when they are derived from regional seismological observations for the area of interest (Regina et al., 2023). For southern Italy it was found that the observed amplitudes decay much faster than global-scale models. This result is confirmed for all the IMs considered (PGV, PGA and SA) observed and modelled in this work and reinforces the indication of using specific datasets when one wants to use GM models for a restricted area.

Acknowledgments

This work was funded by the PRIN2022 project ''Study of active seismogenic sources in the Calabrian arc for an upgrade of the seismic hazard'', CUP H53D23001470006.

References

Bindi D., Pacor F., Puglia R., Massa M., Ameri G., Paolucci R.; 2011: Ground motion prediction equations derived from the Italian strong motion database. Bulletin of Earthquake Engineering. 9. 1899-1920. 10.1007/s10518-011-9313-z.

D'Amico M., Lanzano G., Santulin M, Puglia R., Chiara Felicetta C., Tiberti M., Gomez A. Capera, Russo E.; 2018: Hybrid GMPEs for Region-Specific PSHA in Southern Italy. Geosciences DOI: 10.3390/geosciences8060217.

Lanzano G., Luzi L., Pacor F., Felicetta C., Puglia R., Sgobba S., D'Amico M.; 2019: A Revised Ground-Motion Prediction Model for Shallow Crustal Earthquakes in Italy. Bulletin of the Seismological Society of America 109(2):525-540.

Regina G., Zimmaro P., Taroni M. and Akinci A.; 2023: Peculiar characteristics of ground motion in southern Italy: Insights from, global and regional ground motion models. Earthquake Spectra I-19.

Corresponding author: danilo.galluzzo@ingv.it

Unsupervised Likelihood Inference of the b-Value via Magnitude Differences

C. Godano[1], E. Lippiello[1] and G. Petrillo[2]

[1]*Department of Mathematics and Physics, University of Campania "Luigi Vanvitelli"*
[2]*Earth Observatory of Singapore, Nanyang Technological University, Singapore*

Estimating the Gutenberg-Richter *b*-value (Gutenberg and Richter, 1944) from seismic catalogs is critical for earthquake forecasting and hazard assessment. However, traditional approaches rely on predefined magnitude thresholds and are highly sensitive to catalog incompleteness (Mignan, A. and J. Woessner, 2012), limiting their applicability in automated or real-time settings. We propose a novel, unsupervised inference framework that estimates the b-value directly from the distribution of positive magnitude differences δm, without requiring manual threshold tuning. By introducing a two-parameter probabilistic model, we account for deviations from the ideal exponential form due to spatial and temporal variations in detection capability. This formulation enables a robust and scalable likelihood-based estimation of both the b-value and a correction factor γ, which quantifies incompleteness. We validate our algorithm using synthetic catalogs generated from the ETAS model under varying noise and detection conditions, and apply it to global instrumental datasets from five tectonically active regions. The results demonstrate high accuracy, robustness to incomplete data, and strong potential for integration into machine learning pipelines for seismic monitoring and hazard modeling.

References

Gutenberg B and Richter C; 1944: Frequency of earthquakes in california. Bulletin of the Seismological Society of America 34(4):185–188

Mignan, A. and J. Woessner; 2012: Estimating the magnitude of completeness for earthquake catalogs, Community Online Resource for Statistical Seismicity Analysis, 10.5078/corssa-00180805, http://www.corssa.org

Toward Recognizing the Waveform of Foreshocks

Lippiello[1], G. Petrillo[2], C. Godano[1] and L. Dal Zilio[2,3]

[1]*Department of Mathematics and Physics, University of Campani a "L. Vanvitelli", Caserta, Italy,*
[2]*Earth Observatory of Singapore, Nanyang Technological University, Singapore, Singapore,*
[3]*Asian School of the Environment, NanyangTechnological University, Singapore*

The identification of seismic precursors remains a fundamental challenge (Mignan, 2014; Peng and Lei, 2025). Foreshocks are often indistinguishable from regular seismic sequences, making it difficult to determine whether they precede a larger rupture (Felzer et al., 2004; Petrillo and Lippiello, 2020, 2023). We show that the ground velocity envelope recorded after several Mw6+ foreshocks exhibits an anomalous sawtooth pattern, distinct from typical post-mainshock signals. This pattern suggests the presence of rate-weakening fault patches approaching instability, promoting stress transfer and aftershock migration into neighboring critically stressed regions. A similar signature was observed in multiple events, including the 2011Mw9.1 Tohoku earthquake and the 2014 Mw8.1 Iquique sequence. To assess the systematic occurrence of this anomaly, we introduce an index Q based on the first 45 min of waveform data. Analyzing 68 M6+ earthquakes
in selected regions since 2011, we find that 10 of 11 foreshocks preceding a larger event exhibit anomalous Q values, while only 4 of 57 other events show similar behavior. These findings suggest that foreshock waveform characteristics may provide insight into seismic rupture processes.

References

Mignan, A.; 2014: The debate on the prognostic value of earthquake foreshocks: A meta-analysis. Scientific Reports, 4(1), 4099. https://doi.org/10.1038/srep04099

Peng, Z., Vidale, J. E., Ishii, M., & Helmstetter, A.; 2007 Seismicity rate immediately before and after main shock rupture from high-frequency waveforms in Japan. Journal of Geophysical Research, 112(B3), B03306. https://doi.org/10.1029/2006JB004386

Felzer, K. R., Abercrombie, R. E., and Ekstrom, G.; 2004: A common origin for aftershocks, foreshocks, and multiplets. Bulletin of the Seismological Society of America, 94(1), 88–98. https://doi.org/10.1785/0120030069

Petrillo, G., and Lippiello, E.; 2020: Testing of the foreshock hypothesis within an epidemic like description of seismicity. Geophysical Journal International, 225(2), 1236–1257. https://doi.org/10.1093/gji/ggaa611

Petrillo, G., and Lippiello, E.; 2023: Incorporating foreshocks in an epidemic-like description of seismic occurrence in Italy. Applied Sciences, 13(8), 4891. https://doi.org/10.3390/app13084891

Analytical description of earthquake time interval survival functions

Paolo Harabaglia[1], Giulio Pettenati[2], Teresa Tufaro[3]

[1]Università degli Studi della Basilicata, Potenza

[2]Università degli Studi di Trieste, Trieste

[3]Istituto Nazionale di Geofisica e Vulcanologia, L'Aquila

Earthquake activity in seismic hazard studies is normally assumed to be poissonian. This means that if we consider the relative survival function it is generally considered to be of the form of:

$$P(\tau) = exp - \frac{\tau}{\tau_0}$$

where τ is a specific time interval and $P(\tau)$ refers to the probability that any time interval Δtmight be greater than τ.

This representation is highly unsatisfactory, even though it has the huge advantage to be described by a single parameter τ_0.

In this paper we propose a more general form that describes adequately the survival functions of all the data sets we tested, as long as they are statistically complete.

This form is:

$$P(\tau) = exp - \frac{\tau}{\tau_a + \tau_b \left[0.5 + 0.5erf\frac{\mu + log\tau}{\sqrt{2}\sigma}\right]}$$

where τ_a, τ_b, μ, and σ are parameters that depend on the data set. Unfortunately there seems to be no pattern in these 4 parameters, since the survival function is not stationary even within the same geographical area and magnitude threshold.

An example of the fit is given in Fig. 1 where we show the SF from the ISC-GEM catalogue (Di Giacomo et al., 2018) for the time period 2004-2021 for global events with MW≥6.00 and depth D≤40 km.

We arrived to this formulation by direct inspection, since its form is really straightforward, it is basically a CDF of $log\tau$ shifted and modulated in amplitude.

The importance of this new formulation resides therefore in the possibility to better understand the underlying process more than in modeling the SF.

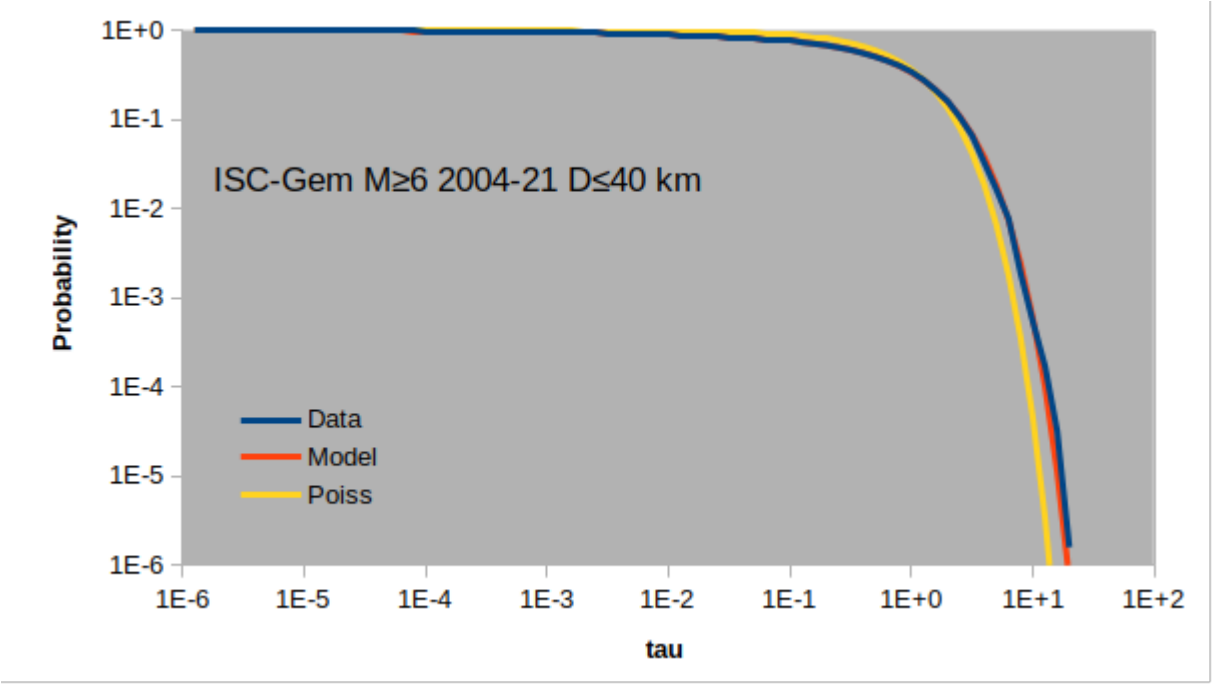

Fig. 1 - Survival function relative to global events with MW≥6.00 and depth D≤40 km in the time period 2004-2021 (blue); the modelled SF according to the new formulation (red); the Poissonian model (yellow).

References

Di Giacomo D., Engdahl E.R. & Storchak D.A.; 2018: The ISC-GEM Earthquake Catalogue (1904–2014): status after the Extension Project, *Earth Syst. Sci. Data*, 10, 1877-1899, https://doi.org/10.5194/essd-10-1877-2018.

Homogenization of the National Earthquake Information Centre (NEIC) magnitudes

Barbara Lolli[1], Daniele Randazzo[1], Paolo Gasperini [1,2]

[1] *Istituto Nazionale di Geofisica e Vulcanologia INGV – Sezione di Bologna*
[2] *Università di Bologna*

In a recent paper we calibrated with respect to moment magnitudes Mw the teleseismic magnitudes mb and Ms of earthquakes reported by the Bulletin of the International Seismological Centre (ISC) at the global scale. The latter includes reviewed events up to about 24 months behind real-time and unreviewed events taken from other agencies, for the remaining 24 months. Most of the unreviewed events provided by ISC come from the National Earthquake Information Centre (NEIC) of the U.S. Geological Survey, which is aimed to provide a Preliminary Determination of Epicenters (PDE) while the ISC Bulletin is the final global archive of parametric earthquake data. However, the NEIC data provided by ISC in near real-time are somehow partial and delayed, hence, to build up a catalog in near real-time of the global seismicity with magnitudes as most homogeneous and complete as possible, it is necessary to acquire the data directly from the NEIC webservices. In this work we present the result of the calibration of NEIC magnitudes as well as a near real-time procedure to download data from NEIC webservices and construct a catalog of global seismicity for time interval not covered by the ISC reviewed Bulletin to be used for seismic hazard assessment and statistical forecasting studies.

Corresponding author: barbara.lolli@ingv.it

Sensitivity of Italian seismic hazard to recent GMMs and microzonation data

F. Sabetta[1], G. Fiorentino[1]

[1] CNR, Institute of Environmental Geology and Geoengineering, Montelibretti RM, 00015, Italy

Introduction

The Italian building code NTC18 (MIT, 2018) is still based on the MPS04 hazard map (Stucchi et al., 2024), which dates back to 2004 and does not incorporate significant advancements in the understanding of seismic sources, seismicity models, and GMMs achieved over the past twenty years. Since 2015, the National Institute of Geophysics and Volcanology (INGV) has coordinated the national scientific community to develop a new seismic hazard model, completed in 2019. However, this new map, known as MPS19, has not yet received official approval (Sabelli, 2023). As a result, although it has been published in a scientific journal (Meletti et al., 2021), the MPS19 data are not yet available in numerical format and therefore cannot be utilized. We therefore considered it useful to assess the changes in the Italian seismic hazard map resulting from the adoption of the most recent Ground Motion Models (GMMs) available in the literature and from the use of new geo-lithological amplification factors derived from microzonation studies (Falcone et al., 2021).

PSHA

In this work, we carried out a Probabilistic Seismic Hazard Assessment (PSHA) of the Italian territory using the same seismotectonic zonation adopted for the MPS04 map (Meletti et al., 2008), updating the earthquake catalogues (Rovida et al., 2011, 2022) and adopting new GMMs. The four GMMs adopted in this study are: ITA10 (Bindi et al. 2011); ASB14 (Akkar et al. 2014); AB10 (Akkar and Bommer 2010), ITA18 (Lanzano et al. 2019). The selection was based on the following criteria: the ranking obtained in the MPS19 study for ITA10 and ASB14; the fit with the Italian building code response spectra for AB10; and the availability of the most recent GMM developed for Italy in the case of ITA18. Fig. 1 shows the response spectra of the selected GMMs compared with those used in the MPS04 study. The four GMMs were combined within a logic-tree framework, with the corresponding weights shown in Fig. 1c.

Results

Fig. 2 compares the Uniform Hazard Spectra (UHS) obtained in this study with those prescribed by the Italian Building Code (IBC) for selected Italian cities.

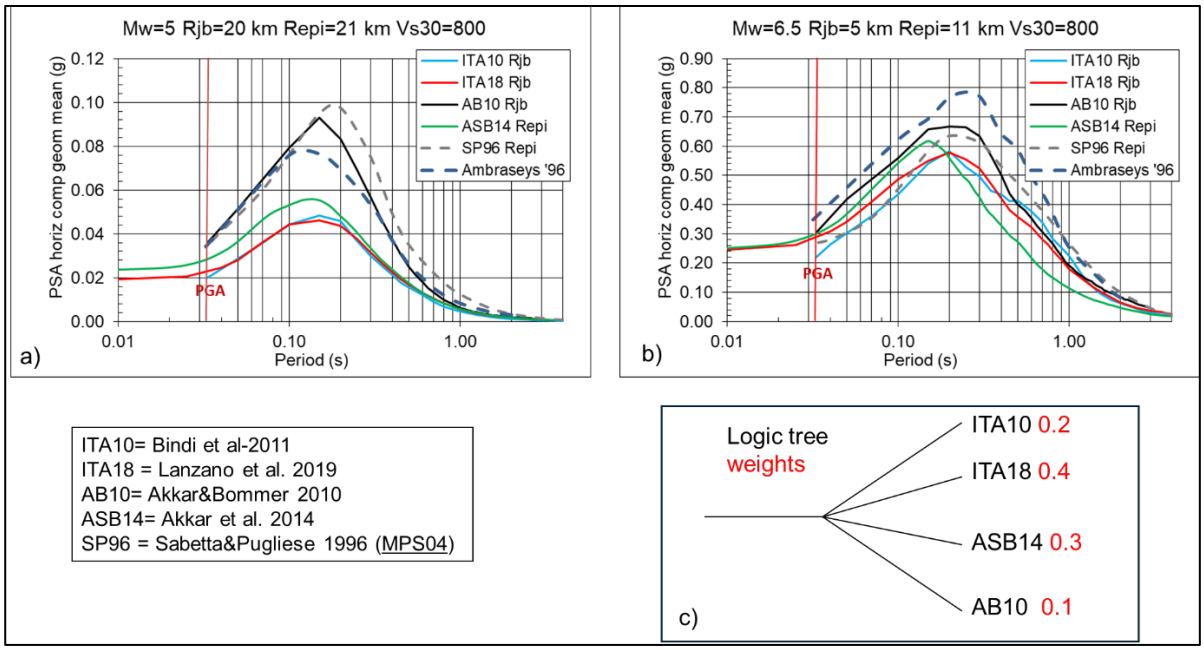

Fig. 1 – Comparison of the elastic response spectra from the four selected GMMs (coloured lines) with those adopted in the MPS04 study (dashed lines): (a) low magnitude and moderate distance; (b) high magnitude and short distance; (c) logic tree and selected weights.

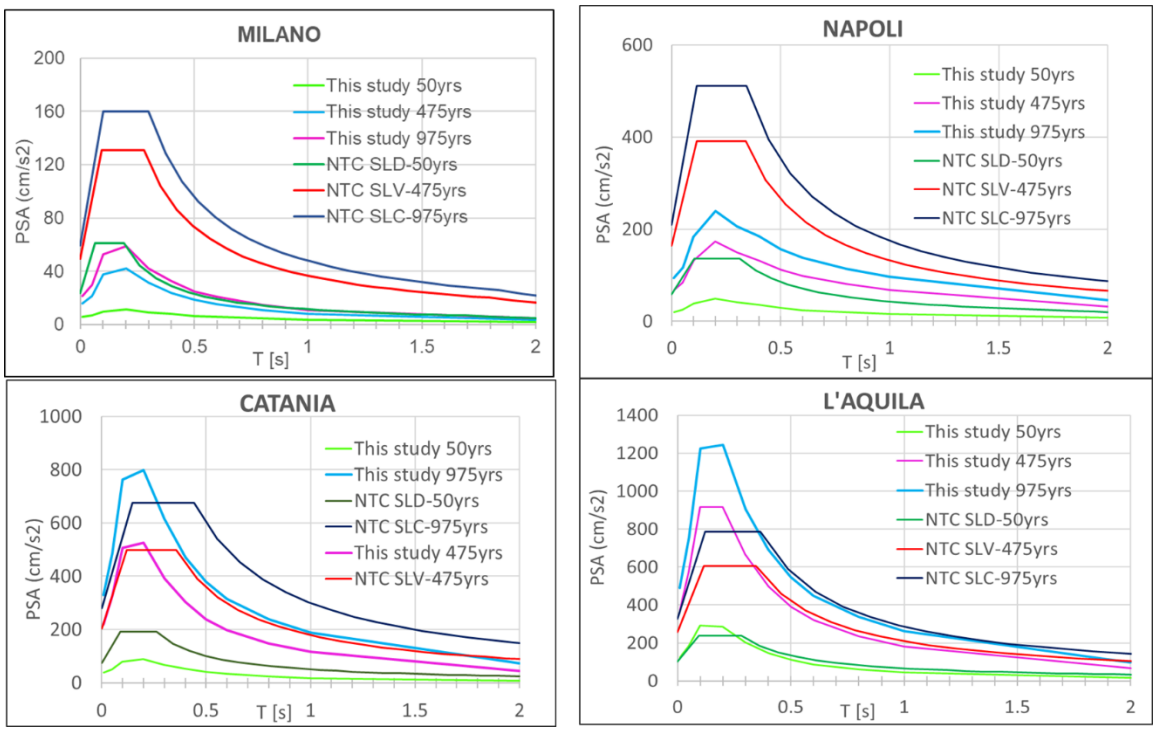

Fig. 2 – Comparison of the UHS obtained in this study with those prescribed by the Italian building code, for different return periods, for selected Italian cities.

For short return periods (50 years), the UHS are lower than the IBC spectra over the entire range of structural periods considered (0–2 s). For longer return periods (475 and 975 years), the UHS exceed the IBC values—particularly at short spectral periods—in municipalities characterized by

high seismicity (e.g., Catania and L'Aquila), while they are quite lower than the IBC spectra in areas of low seismicity (e.g., Milan and Naples).

Fig. 3 shows the percentage difference between the hazard values calculated in this study and those of the MPS04 map. For PGA (Fig. 3a), the new estimates are higher—by up to 67%—than those of MPS04 along the entire Apennine chain and, more generally, in central and southern Italy. The highest PGA increases from 0.28 g in Ferla (Siracusa) to 0.43 g in Pietraroja (Benevento). Conversely, in large parts of northern Italy and in some coastal areas, a decrease in PGA of up to 86% is observed. For response spectral values at a period of 1 second (Fig. 3b), the new estimates show a generalized decrease across the entire Italian territory, with the exception only of the highest seismicity area in Irpinia (seismogenic zone no. 927). These patterns result from the differences between the old and new GMMs, as illustrated in Fig. 1.

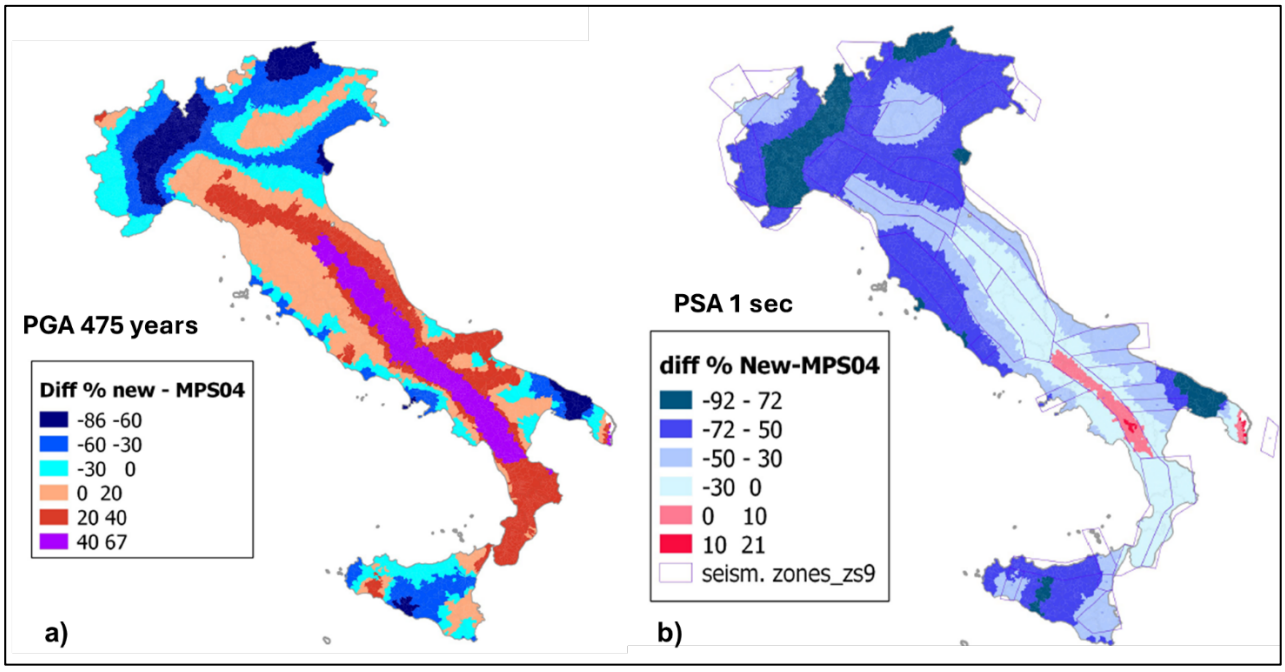

Fig. 3 – Percentage difference between the hazard values calculated in this study and those of the MPS04 map. Hazard values (rocky type of soil) are assigned to the main town of each of the 7,715 Italian municipalities (excluding Sardinia): (a) PGA; (b) pseudo-spectral acceleration at a period of 1 second.

The geo-lithological amplification factors have been taken from the study of Falcone et al. (2021) based on the new VS30 map from the work of Mori et al. (2020) using a large amount of data from the Italian seismic microzonation. The introduction of site amplification factors results in an average increase in PGA of 76%, with Pontelandolfo (Benevento) becoming the municipality with the highest PGA (0.73 g)

Conclusions

Probabilistic Seismic Hazard maps of Italy have been developed using updated earthquake catalogues and new GMMs compared to those adopted in the currently enforced MPS04 map.

Only minor differences are attributable to the catalogue updates, particularly in volcanic areas where specific GMMs were applied (Iervolino, 2024). The main differences with respect to the MPS04 map are due to four recent GMMs arranged in a logic tree, resulting in an increase of ground spectral acceleration at short periods in central and southern Italy, with the exception of some areas (e.g., Naples, central Sicily). Conversely, a considerable decrease in spectral accelerations at periods longer than 0.3 seconds is observed, particularly in northern Italy. The inclusion of site-specific geomorphological amplification factors derived from microzonation studies leads to an average PGA increase of 76%

References

Akkar S., J.J. Bommer (2010). Empirical equations for the prediction of PGA, PGV, and spectral accelerations in Europe, the Mediterranean region, and the Middle East, Seismol. Res. Lett., 81(2), 195-206.

Akkar S., M.A. Sandıkkaya, J.J. Bommer (2014). Empirical ground-motion models for point- and extended-source crustal earthquake scenarios in Europe and the Middle East, Bull. Earthq. Eng., 12(1), 359–387.

Ambraseys NN, Simpson KA, Bommer JJ (1996) Prediction of horizontal response spectra in Europe. Earth Eng Struct Dyn 25:371–400.

Bindi D., F. Pacor, L. Luzi, R. Puglia, M. Massa, G. Ameri, R. Paolucci (2011). Ground motion prediction equations derived from the Italian strong motion database, Bull. Earthq. Eng., 9(6), 1899–1920.

Falcone G., Acunzo G., Mendicelli A., Mori F., Naso G., Peronace E., Porchia A., Romagnoli G., Tarquini E., Moscatelli M. (2021) Seismic amplification maps of Italy based on site-specific microzonation dataset and one-dimensional numerical approach. Engineering Geology 289:1-25. https://doi.org/10.1016/j.enggeo.2021.106170

Lanzano, G., Luzi, L., Pacor, F., Felicetta, C., Puglia, R., Sgobba, S., & D'Amico, M. (2019). A revised ground-motion prediction model for shallow crustal earthquakes in Italy. Bulletin of the Seismological Society of America, 109(2), 525-540.

Iervolino I.,Cito P.,De Falco M.,Festa G.,Herrmann M.,Lomax,A,Marzocchi W., Santo A.,Strumia C., Massaro L.,Scala, A.,Scotto di Uccio F.,Zollo A (2024) Seismic risk mitigation at Campi Flegrei in volcanic unrest. Nat Commun 15, 10474, https://doi.org/10.1038/s41467-024-55023-1.

Meletti C., Galadini F., Valensise G., Stucchi M., Basili R., Barba S., Vannucci G., Boschi E. (2008) Zonazione sismogenetica ZS9. Istituto Nazionale di Geofisica e Vulcanologia (INGV), https://doi.org/10.13127/sh/zs9

Meletti, C., Marzocchi, W., D'amico, V., Lanzano, G., Luzi, L., Martinelli, F., ... & Seno, S. (2021). The new Italian seismic hazard model (MPS19). Annals of Geophysics, 64(1).

MIT (2018), Ministero Infrastrutture e Trasporti. NTC18. Aggiornamento delle Norme Tecniche per le Costruzioni (Decreto Ministeriale 17-01-2018) e Istruzioni per l'applicazione delle NTC2018, Gazzetta ufficiale n. 35 dell'11-02-2019..

Mori F, Mendicelli A, Moscatelli M, Romagnoli G, Peronace E, Naso G (2020) A new VS30 map for Italy based on the seismic microzonation dataset. Eng Geol 275:1–10. https://doi.org/10.1016/j.enggeo.2020.105745.

Rovida A., Camassi R., Gasperini P. e M. Stucchi (2011). Catalogo Parametrico dei Terremoti Italiani (CPTI11), INGV, https://doi.org/10.6092/INGV.IT-CPTI11

Rovida A., Locati M., Camassi R., Lolli B., Gasperini P., Antonucci A. (2022). Italian Parametric Earthquake Catalogue (CPTI15), version 4.0, INGV, https://doi.org/10.13127/cpti/cpti15.4

Sabelli, C (2023). "Italy's new seismic hazard map is back to square one." Nature Italy, https://www.nature.com/articles/d43978-023-00072-1.

Sabetta F, Pugliese A. (1996) Estimation of response spectra and simulation of nonstationary earthquake ground motions. Bull Seismol Soc Am 86(2):337–352.

Stucchi M, Akinci A, Faccioli E, Gasperini P, Malagnini L, Meletti C, Montaldo V, Valensise G. (2004) MPS04 Mappa di Pericolosità sismica del territorio Nazionale. http://zonesismiche.mi.ingv.it/documenti/rapporto_conclusivo.pdf.

Corresponding author: fabio.sabetta@uniroma3.it

Exploring Fault Behaviour and Seismic Hazard in the Central Apennines through Earthquake Simulations

Khatereh Saghatforoush[1], Bruno Pace[1], Alessandro Verdecchia[2], Francesco Visini[3], Octavi Gomez Novell[4], Olaf Zielke[5], Laura Peruzza[6]

[1] Università degli Studi "G. d'Annunzio" Chieti-Pescara, Italy
[2] Ruhr-University Bochum, Germany
[3] Istituto Nazionale di Geofisica e Vulcanologia INGV, Italy
[4] CN Instituto Geologico y Minero de Espana, Madrid, Spain
[5] KAUST, Thuwal, Saudi Arabia
[6] Istituto Nazionale di Oceanografia e di Geofisica Sperimentale –OGS, Italy

The Central Apennines (Italy) are characterized by moderate seismicity and active fault systems capable of generating damaging earthquakes. However, the limited duration of historical and paleoseismic records restrict our understanding of long-term fault behaviour. In this study, we use the Multi-Cycle Earthquake Rupture Simulator (MCQsim; Zielke and Mai, 2023) to construct a 3D model of 42 active normal faults and to generate multiple 100,000-year-long synthetic earthquake catalogues. We systematically vary key model parameters, including dynamic friction and fault strength heterogeneity, to assess their influence on earthquake occurrence rates, magnitude-frequency distributions, and rupture scaling.

The simulations reproduce the regional Gutenberg–Richter trend and show magnitude–average slip and magnitude–rupture area relationships consistent with empirical scaling laws and the available historical catalogue. Seismic productivity and rupture characteristics are most sensitive to variations in dynamic friction and fault heterogeneity. Although uncertainties arise from simplified fault geometries and assumptions about seismogenic depth, the overall agreement between synthetic and observed seismicity suggests that MCQsim effectively captures key aspects of long-term fault-system behaviour. These results indicate that physics-based synthetic earthquake catalogues can improve constraints on earthquake recurrence and rupture scenarios, providing valuable input for probabilistic seismic hazard assessment in regions characterized by moderate seismicity, complex active fault systems, and sparse observational data.

References

Zielke O. and Mai M. (2023) – MCQsim: a multicycle earthquake simulator, Bulletin of the

Seismological Society of America, 113-3, 889-908.

Corresponding author: khatereh.saghatforoush@phd.unich.it

A concise but structured overview of the evolution of the DISS database: an AI perspective

G. Valensise

Istituto Nazionale di Geofisica e Vulcanologia (INGV)

A meeting of seismologists held in Udine on the 50th anniversary of the devastating 1976 Friuli earthquake is indeed an opportunity to draw a balance of how much we have progressed in the understanding of seismogenic processes, and specifically on the role of geological observations and methods in anticipating the characteristics of future earthquakes.

When the 1976 earthquakes occurred, the Italian community of scientists concerned with active tectonics, seismotectonics and seismic hazard had just started looking for active faults in relation with large earthquakes. The earthquake had catastrophic consequences for the built environment but did not cause clear and undisputable geological and environmental effects: once more, the *rationale* of the different shocks was revealed by seismological and geodetic data.

In those years, the main contribution of the geological community to assessing seismic hazard in most European countries usually included the identification of “Quaternary faults” (sometimes called “Neotectonic faults”) and the preparation of fault maps, generally at regional if not national scale. The seismologically-detected sources of the 1976 shocks were consistent with some of the mapped Quaternary faults, but was not satisfactory for most of the geologists concerned. Assigning *ex-post* a (large) earthquake to a recognized (large) active fault could perhaps be seen as a confirmation of the seismogenic potential of tha anticipate the large earthquakes of the future, and this could hardly be achieved on the basis of a lat particular fault: but the goal of Quaternary geologists and seismotectonicists is primarily torge set of Quaternary faults only. There were at least three main limitations, which are somehow inherent to the culture and to the perspective of field geologists:

a) they have limited access to subsurface geology; this implies that

b) they have a hard time hierarchizing the active faults they detect, plus

c) the sources of many earthquakes are buried (blind), or somehow hidden, or offshore.

In the late 1990’s, following the 1997 Colfiorito, central Italy, earthquakes, a group of ING (later INGV) scientists proposed to overcome these limitations by reversing the current paradigm and identifying not just faults, but *seismogenic sources*, i.e. fault systems responsible for/capable of generating earthquakes of magnitude 5.5 and larger. They did it by blending geological and

geophysical information with instrumental and macroseismic data. This contamination was inevitable if we were to overcome all three limitations outlined above; plus, formalizing seismogenic sources was the only way to make geological information useful for actually calculating – not just guessing – seismic hazard. Up to that moment these calculations were essentially based on historical seismicity, in the attempt to project the past into the future: this is indeed one of the sacred principles of Geology, but past earthquakes do not say much about the geological processes which generated them. The introduction of seismogenic sources was the only way to look straight into the future of a region's or a nation's seismic hazard.

In the year 2000, the prototype of the Database of Individual Seismogenic Sources (DISS v. 1.0) was borne out of these principles, ideas and hard-to-achieve goals. For many large eartquakes of the past and of the future, DISS shifted the focus from vaguely defined earthquake epicenters to the identification of the earthquake causative source, represented by a simplified 3D plane. In 2025, a quarter of a century later, its v. 3.3.1 retains all basic principles and scopes of that original version, but features a more articulated structure, more parameters and tools, and a much larger number of seismogenic sources and bibliographic references.

DISS was conceived as a necessary step toward a fault-based seismic hazard framework, aligned with international developments in seismic source characterization. DISS was designed to emphasize consistency, transparency, and reproducibility in the criteria for defining seismogenic sources and in the definition of their parameters and uncertainties. Perhaps more importantly, it was designed as a true scientific database, where any piece of information provided is backed by data, reasoning and literature references, making assumptions and uncertainties explicit: not just as stack of faults defined only by their 2D shape, something the modern machine-learning techniques could do automatically.

Did the initiators of the DISS database succeed? As a veteran of the DISS Working Group, I have a professional and moral obligation to abstain from answering this question myself . But I decided to let an independent, intelligent, adaptive, extremely powerful and smart pal answer for me: *he/she* is called ChatGPT. I will show you what *he/she* thinks about the evolution of the DISS database, and *he/she* will tell us all whether or not we achieved our original goals.

Corresponding author: gianluca.valensise@ingv.it

An Algorithm for Rupture Catalog Generation in Complex Fault Systems: Integrating 3D Geometry and Depth-Dependent Constraints

A. Valentini[1]

[1] *Department of Geology, University of Vienna, Austria*

1. Introduction

Probabilistic Seismic Hazard Analysis (PSHA) relies on the definition of all physically plausible rupture scenarios across a given fault system. Traditional PSHA models, particularly those based on the floating rupture or segmentation approaches, often simplify fault geometry into 2D linear geometry. This simplification leads to limitations when dealing with naturally occurring complex and irregular fault geometries, such as non-planar faults, segmented systems, or branched ('Y' or 'T' shaped) networks. For example, simplified approaches cannot accurately implement constraints that are non-uniform, such as depth-dependent connectivity criteria. The crust's mechanical behavior differs significantly between the brittle, shallow layer (0-5 km) and the deeper, semi-brittle layer (5-15 km), requiring dynamic geometric filters. This work introduces an algorithm designed to overcome these limitations and systematically define a comprehensive catalog of all possible ruptures in complex fault networks starting from a magnitude forecast.

The proposed algorithm replaces the concept of a linear fault system with a detailed 3D mesh of interconnected sub-sections, using a hierarchical filtering process to define plausible rupture scenarios. The first tier utilizes traditional, fast geometric checks to define coarse "fault groups" or physically independent networks. This step leverages a maximum absolute gap constraint and optional kinematic filters (e.g., maximum difference in mean rake angle) to dramatically reduce the computational domain, ensuring that only geographically and kinematically related faults are processed together in the subsequent, high-resolution tier.

2. Depth-Dependent filtering

The core of the methodology lies in the accurate geometric discretization of the system. Based on the forecast magnitude, each fault is divided into a regular grid of m sub-sections, and the 3D coordinates (X, Y, Z) of the centroid for every single sub-section are calculated based on the fault's strike, dip, and dip-direction derived from the surface trace.

This information is used to build a sparse adjacency matrix, where an entry $Aij=1$ if sub-section i is connected to sub-section j. The connection criteria are defined by two sets of rules:

1. Internal Connectivity: Sub-sections within the same parent fault are connected only if they share an orthogonal border (i.e., excluding diagonal connections), ensuring that the elementary rupture unit is a perfect rectangle in the index space.
2. External Connectivity (Inter-Fault): Sub-sections belonging to different faults are connected only if they satisfy advanced physical constraints.

A key innovation in defining external connectivity is the implementation of a depth-dependent physical gap constraint. This ensures the completeness of the rupture catalog by accounting for the inherent mechanical and geometrical uncertainties in the deeper crust. The permissible 3D distance between the centroids of two connecting sub-sections is dynamically controlled by their mean reference depth. In this way, for shallow regions, a strict geometric filter can be enforced. This reflects the rigidity and high-resolution constraint derived from surface data. For deeper regions, the filter can be significantly relaxed to allow for mechanically plausible larger jumps. This relaxation captures the greater uncertainty regarding true fault proximity at depth and acknowledges the potential for enhanced mechanical coupling and rupture propagation through broader damage zones in the semi-brittle crust. Moreover, this layered approach guarantees that ruptures separated by large horizontal distances at the surface but likely connected through complex structures or broader zones of localized deformation at depth, are not arbitrarily excluded.

3. Rupture Generation and Combination Scheme

The rupture catalog is generated using a two-stage combinatorial approach that preserves geometric integrity while allowing multi-fault complexity:

Phase I: *Elementary Rectangular Rupture Generation:* within each fault group, all possible elementary ruptures are defined. An elementary rupture must be a contiguous block (a perfect rectangle) in the local sub-section index space. All elementary ruptures are filtered by a strict Aspect Ratio (AR) constraint to exclude elongated or implausible shapes. These valid rectangles form the nodes of the subsequent combination graph.

Phase II: *Multi-Fault Combination***:** the final rupture catalog is built by combining these elementary rectangular ruptures from different faults within the same group. For example, in a simple system made by two faults, two rectangles are combinable if at least one sub-section belonging to the physical boundary of the first fault is connected to at least one sub-section on the physical boundary of the second fault.

Each combined rupture is subjected to a final check on its total area, resulting moment magnitude, and the overall AR of the combined polygon.

4. Conclusions

The proposed methodology successfully addresses the limitations of linear rupture models. By moving the core decision-making process from the linear index space to the high-resolution 3D physical space, this algorithm ensures that: 1) rupture propagation across complex geometries (e.g., 'Y' bifurcations) is only permitted where physical proximity and kinematic compatibility are met (eliminating non-physical jumps), 2) geometrical integrity is maintained within single faults

(rectangle constraint), and 3) the physical constraints on connectivity can reflect the varying mechanical properties of the crust with depth.

The resulting rupture catalog provides a more physically rigorous and comprehensive basis for next-generation fault-based PSHA, particularly for seismically active regions characterized by dense and geometrically complex fault networks. The approach is generalizable and easily adaptable to different regional tectonic settings by tuning all filters and constraints.

Acknowledgements

This work was carried out within the framework of the Austrian Science Fund (FWF) project NEXTQUAKE (Project no.: PAT 2160424, Grant-DOI: 10.55776/PAT2160424).

Corresponding author: alessandro.valentini@univie.ac.at

New insights into temporal changes in magnitude probability distribution in Central Italy

Elisa Varini[1], Renata Rotondi[1], Alex González Fuentes[1]

[1] *Consiglio Nazionale delle Ricerche, Istituto di Matematica Applicata e Tecnologie Informatiche CNR-IMATI, Milano, Italy*

Non-extensive Statistical Mechanics (NESM) extends classical Boltzmann–Gibbs physics through Tsallis entropy (Tsallis, 2009), introducing the *q-exponential* distribution to better model long-range correlations and dynamics of complex systems. This approach is well suited for earthquakes: it is intrinsically complex, spans spatial scales from microcracks to major fault zones and temporal scales from seconds to centuries, despite it exhibits robust statistical features such as power-law distributions for magnitude and aftershock decay, and multifractal epicenter clustering. In this framework, by maximizing Tsallis entropy and applying the fragment-asperities interaction model (Sotolongo-Costa and Posadas, 2004), the *q-exponential* magnitude distribution is obtained, reducing to the classical exponential Gutenberg–Richter law as q approaches 1.

In Rotondi et al. (2022), we examined real seismic sequences: we derived the *q-exponential* magnitude distribution and analyzed the L'Aquila and Amatrice–Norcia sequences, covering the periods 2005-2009 and 2014-2018, respectively, to assess how their magnitude distributions changed before and during the seismic crises. Temporal variations in Tsallis entropy and in the q index of the corresponding *q-exponential* distribution are estimated using sliding windows of a fixed number of events, advancing one event at a time, and applying Bayesian inference via the MCMC methods (Rotondi et al., 2025). We found a link between variations in the estimated q-index values and phases of seismic crises, with low q values potentially indicating the onset of strong events.

In the present study, we combine all events recorded in the region from 2005 to 2024, using the most complete section of the ISIDe catalog, and examine them as a unified sequence. Our goal is to determine whether the temporal variations detected in Tsallis entropy and in the estimated q entropic index in the previous works truly act as both sufficient and necessary precursory signals of strong earthquakes. Results show that a significant and persisting reduction of entropy and of the q parameter, index of energy concentration, could be considered as a necessary but not sufficient condition for the occurrence of a strong seismic shock. However, taking into account that the *q-exponential* distribution has, in addition to q, another parameter β related to the volumetric energy density, we observe that the joint analysis of q and β and of their correlation provides a more reliable identification of periods of impending heightened seismic activity.

For comparison, we also analyzed the region's seismicity over the same period using the HORUS catalog, which provides an accurate and consistent assessment of the moment magnitude for all recorded events, and obtained consistent results.

Acknowledgments

This research is supported by ICSC National Research Centre for High Performance Computing, Big Data and Quantum Computing (CN00000013, CUP B93C22000620006) within the European Union-NextGenerationEU program.

References

Rotondi, R., Bressan, G., Varini, E.; 2022: Analysis of temporal variations of seismicity through non-extensive statistical physics, Geophys. J. Int. Vol. 230, n. 2, 1318-1337, https://doi.org/10.1093/gji/ggac118

Rotondi, R., Nicolis, O., Varini, E., Ruggeri, F.; 2025: Variations in Probability Distributions as Indicators of Seismic Phases: A Case Study from Chile. Seismol. Res. Lett. Vol. 96, n. 4, 2587-2602, https://doi.org/10.1785/0220240240

Sotolongo-Costa, O., Posadas, A.; 2004: Fragment-asperity interaction model for earthquakes. Phys. Rev. Lett. Vol. 92, n. 4, https://doi.org/10.1103/PhysRevLett.92.048501

Tsallis, C.; 2009: Introduction to nonextensive statistical mechanics. approaching a complex world. Springer, Berlin

Corresponding author: elisa@mi.imati.cnr.it

Stability of the Gela Basin Margin and Tsunamigenic Potential of Submarine Landslides in the Sicily Channel

M. Zanetti[1], F. Zaniboni[1], C. Angeli[1], E. Paolucci[1], A. Armigliato[1], M. Rovere[2], A. Argnani[2]

[1] Department of Physics and Astronomy "A. Righi", Alma Mater Studiorum - University of Bologna, Bologna, Italy
[2] ISMAR – CNR, Bologna, Italy

In recent years, a growing body of research has focused on the interaction between offshore activities and natural hazards, particularly in areas characterized by active tectonics and submarine slope instabilities and located close to strategic coastal settlements and infrastructures. The present work is developed within the framework of the SPIN Project ("Test delle Buone Pratiche per lo studio della potenziale interazione tra attività offshore e pericolosità naturali", in english "Test of good practices for the study of potential interaction between offshore activities and natural hazards"), funded by the Italian Ministry of Environment and Energy Security (MASE). The project ended in October 2025 and involved various Italian Research Institutes, Universities, and Public Administrations. The main objective of the project was to develop and test a workflow for the analysis of offshore natural hazards that could interact with offshore hydrocarbon exploitation, with particular emphasis on potentially triggered seismicity, its cascading effects—such as earthquake- and landslide-generated tsunamis—and their impacts on coastal and inland areas. The SPIN project concerned two study areas located in the northern Adriatic Sea and the Sicily Channel. In this contribution, we focus on the latter which develops along the Gela Basin, an area located south of the Gulf of Gela and marked by the widespread evidence of past submarine mass movements and by the proximity of densely populated coastal zones and industrial facilities (e.g., Gauchery et al., 2021; Zaniboni et al., 2021).

The adopted workflow combines geomorphological reconstruction of submarine landslides, stability analysis, dynamic modeling of landslide motion, and numerical simulations of tsunami generation, propagation, and coastal inundation. Six landslide scenarios were reconstructed along the Gela Basin—Northern Twin Slide (NTS), Southern Twin Slide (STS), Serenusa Slide (SER), Vigata Slide (VIG), South Gela Basin Slide (SGBS), and Gela Drift Slide (GDS)—using constraints derived from bathymetric data, which allowed the morphometric mapping of detachment scars and depositional bodies.

Slope stability was investigated using the LEM-MLD approach, i.e., a Limit-Equilibrium Method (LEM) formulation based on the Minimum Lithostatic Deviation (MLD) principle, originally developed by Tinti and Manucci (2006, 2008). In this framework, the factor of safety is evaluated within a minimization-based scheme, providing an alternative to classical LEM formulations. Seismic loading was accounted for in terms of peak ground acceleration (PGA), estimated for each scenario by considering three offshore possible seismogenetic sources (named "Gela11", "Pozzallo30", and "Pozzallo36", described in a companion presentation by Angeli et al., 2026). PGA

was computed using the ITA10 ground-motion prediction model proposed for the Italian region (Bindi et al., 2011).
To evaluate the impact of uncertainties on stability outcomes, a global sensitivity analysis was performed using variance-based Sobol indices (Saltelli and Sobol, 1995). The analysis was first performed by considering geotechnical parameters only, and subsequently extended to include seismic loading among the uncertain inputs, allowing the combined effects of material properties and ground-motion variability to be evaluated.
Landslide dynamic was simulated using the UBO-BLOCK model (Tinti et al., 1997), and the resulting time-dependent seafloor deformation was translated into a tsunamigenic impulse through the intermediate code UBO-TSUIMP (Tinti et al., 2006). Tsunami generation, propagation, and coastal inundation were then simulated using the JAGURS software (Baba et al., 2015). Given the characteristics of landslide-generated tsunamis, dispersive effects were explicitly accounted for in all simulations. A non-linear formulation was adopted to properly represent nearshore processes and coastal inundation. Tsunami simulations were performed on a system of nested grids, allowing the analysis of both basin-scale propagation and localized effects in bays and harbor areas.

The stability analyses indicate that the majority of the submarine landslides are stable under the considered loading conditions, while only a limited number of scenarios (i.e., NTS and STS) show clear instability. Sensitivity analyses indicate that, among geotechnical parameters, the friction angle exerts the strongest control on slope stability, whereas when seismic loading is included among the uncertain inputs, PGA becomes the dominant controlling factor.
Tsunami simulations show that the propagation in coastal areas is mostly controlled by local bathymetry and coastal morphology. The geometry of the Gulf of Gela and its relatively wide and shallow continental shelf plays a key role in trapping and redistributing tsunami energy, resulting in spatially heterogeneous coastal responses that are not necessarily correlated with the distance from the tsunami source.
High-resolution simulations further highlight the importance of wave interaction with coastal features such as bays and harbor basins, where resonance phenomena may develop depending on both basin geometry and wave characteristics. In some cases, longer-period oscillations are also observed, suggesting the occurrence of more complex nearshore processes related to coastal trapping and basin-scale responses.

References

Baba T., Takahashi N., Kaneda Y., Ando K., Matsuoka D., Kato T.; 2015: Parallel implementation of dispersive tsunami wave modeling with a nesting algorithm for the 2011 Tohoku tsunami. Pure appl. Geophys., doi:10.1007/s00024-015-1049-2, 2015.

Bindi D., Pacor F., Luzi L., Puglia R., Massa M., Ameri G., Paolucci R.; 2011: Ground motion prediction equations derived from the Italian strong motion database. Bulletin of Earthquake Engineering, 9(6), 1899-1920.

Gauchery T., Rovere M., Pellegrini C., Cattaneo A., Campiani E., Trincardi F.; 2021: Factors controlling margin instability during the plio-quaternary in the Gela Basin (Strait of Sicily, Mediterranean Sea). Mar. Petrol. Geol., 123, 104767. DOI: 10.1016/j.marpetgeo.2020.104767.

Saltelli A., Sobol' I. M.; 1995: Sensitivity analysis for nonlinear mathematical models: numerical experience. Matematicheskoe Modelirovanie, 7(11), 16–28.

Tinti S., Bortolucci E., Vannini C.; 1997: A block-based theoretical model suited to gravitational sliding. Natural Hazards, 16, 1-28.

Tinti S., Manucci A.; 2006: Gravitational stability computed through the limit equilibrium method revisited, Geophys. Int. J. 164: 1-14.

Tinti S., Manucci A.; 2008: A new computational method based on the minimum lithostatic deviation (MLD) principle to analyse slope stability in the frame of the 2-D limit equilibrium theory, Nat. Hazards Earth Syst. Sci. 8: 671-683.

Tinti S., Pagnoni G., Zaniboni F.; 2006: The landslides and tsunamis of 30th December 2002 in Stromboli analysed through numerical simulations. Bulletin of Volcanology, 68, 462-479. DOI: 10.1007/s00445- 005-0022-9.

Zaniboni F., Pagnoni G., Paparo M.A., Gauchery T., Rovere M., Argnani A., Armigliato A., Tinti S.; 2021: Tsunamis from Submarine Collapses along the Eastern Slope of the Gela Basin (Strait of Sicily). Front. Earth Sci. 8, 602171. https://doi.org/10.3389/feart.2020.602171.

Corresponding author: martina.zanetti8@unibo.it

Onshore seismic stations as meteotsunami sensors: integrated analysis of seismic, meteo-marine and satellite data of the May 2017 Sicily Channel event, Italy

S. Zappalà[1], S. D'Amico[1,2], A. Cannata[1,3], F. Panzera[1]

[1]*Università di Catania, Dipartimento di Scienze Biologiche, Geologiche e Ambientali, Sezione di Scienze della Terra, Catania, Italia*
[2]*Istituto Nazionale di Geofisica e Vulcanologia, Sezione Roma2, Roma, Italia*
[3]*Istituto Nazionale di Geofisica e Vulcanologia, Osservatorio Etneo, Catania, Italia*

Meteotsunamis are tsunami-like long ocean waves generated by atmospheric disturbances that can produce sudden sea-level oscillations and coastal damage comparable to seismic tsunamis (Monserrat et al., 2006; Vilibić et al., 2021). Their amplification depends critically on coastal resonant mechanisms, such as Proudman resonance over continental shelves and alongshore Greenspan resonance in elongated bays (Proudman, 1929; Greenspan, 1956; Miles & Munk, 1961). In the central Mediterranean, tsunami early-warning systems exist which remain sensitive to uncertainties in the speed and track of the atmospheric disturbance, and effective nowcasting requires minute-scale sea-level and pressure measurements (Šepić et al., 2012; Denamiel et al., 2019; Tojčić et al., 2021). Coastal broadband seismic stations located close to the shoreline can record the associated long-period ground motion, with energy in the millihertz band, providing an independent constraint on meteotsunami timing and propagation (Okal, 2021; D'Amico et al., 2025).

The Sicily Channel is one of the most meteotsunami-prone regions in the Mediterranean area, owing to its wide, shallow continental shelf and its favourable position for the development and guidance of intense convective systems (Candela et al., 1999). Within this region, the harbour of Lampedusa is particularly exposed: its semi-enclosed basin behaves as a resonant box, enhancing harbour resonance and amplifying sea-level oscillations (Vilibić et al., 2008; Rabinovich, 2009; Šepić et al., 2012; Vilibić et al., 2016).

This study combines integrated seismic, meteo-marine and satellite data to characterize the severe meteotsunami event that struck Lampedusa Island during the night between 11th and 12th May 2017.

Broadband seismic data from Lampedusa, Malta and south-eastern Sicily were corrected for the instrument response to obtain ground displacement and bandpass-filtered between 0.1-10 mHz to isolate the characteristic meteotsunami signal. Through the analysis of the seismic signal based on Root Mean Square (RMS) amplitude, we were able to construct the spatio-temporal progression of the low pressure front that generated the meteotsunami event.

For meteorological and marine observations, we used sea level and barometric data from three stations of the National Tide Measurement Network managed by ISPRA, located at Sciacca, Porto Empedocle and Lampedusa along the southern Sicilian coast. A harmonic analysis was performed on the sea level data in order to reconstruct the astronomical tide and calculate the residuals. Finally, both the sea level residuals and the pressure data were filtered in the meteotsunami frequency band range.
Lampedusa showed the clearest response, with sea-level residuals up to ~0.5 m between late 11th May and the early hours of 12th May, anticorrelated with a local pressure drop, a typical meteotsunami signature. At Sciacca and Porto Empedocle, no single peak matched the Lampedusa amplitude, but enhanced oscillations co-occurred with pressure falls; residuals remained modest at Sciacca, whereas more abrupt fluctuations at Porto Empedocle on the morning of 12th May were consistent with a weaker meteotsunami response.

ERA5 reanalysis fields (Hersbach et al., 2020) depict a mesoscale atmospheric disturbance crossing the Sicily Channel during the event, characterized by cooling at 850 hPa, strengthened mid-tropospheric winds, and a surface low consistent with the observed marine and seismic signatures. Our results demonstrate that onshore broadband seismic stations act as effective complementary sensors for meteotsunami detection and that integrating seismic, oceanographic, and atmospheric observations improves reconstruction of propagation dynamics and supports the design of new multiparametric early-warning strategies in the central Mediterranean.

References

Candela, J., Mazzola, S., Sammari, C., Limeburner, R., Lozano, C. J., Patti, B., & Bonnano, A.; 1999: The “Marrobbio” in the Strait of Sicily. *Journal of Physical Oceanography*, *29*(9), 2210–2231. https://doi.org/10.1175/1520-0485(1999)029<2210:TMITSO>2.0.CO;2

D’Amico, S., Cannata, A., Panzera, F., & Marinaro, G.; 2025: Seismic reconstruction of meteotsunami wave heights using coastal seismic stations: an application in the Port of Hamina, Gulf of Finland. *Natural Hazards*, 1-18. https://doi.org/10.1007/s11069-025-07407-9

Denamiel, C., Tojčić, I., Šepić, J., & Vilibić, I., 2019; Performance of atmosphere-ocean coupled and uncoupled numerical models in simulating Adriatic meteotsunamis. *Progress in Oceanography*, *175*, 205–223. https://doi.org/10.1016/j.pocean.2019.04.004

Greenspan, H. P.; 1956: The generation of edge waves by moving pressure distributions. *Journal of Fluid Mechanics*, *1*(6), 574–592. https://doi.org/10.1017/S0022112056000344

Hersbach, H., Bell, B., Berrisford, P., Hirahara, S., Horányi, A., Muñoz-Sabater, J., Peubey, J., Radu, R., Schepers, D., Simmons, A., Soci, C., Thepaut, J., & Vitart, F.; 2020: The ERA5 global reanalysis. *Quarterly Journal of the Royal Meteorological Society*, *146*(730), 1999–2049. https://doi.org/10.1002/qj.3803

Miles, J. W., & Munk, W. H.; 1961: Harbor paradox. *Journal of Waterways and Harbors Division*, *87*(3), 111–130.

Monserrat, S., Vilibić, I., & Rabinovich, A. B.; 2006: Meteotsunamis: Atmospherically induced destructive ocean waves in the tsunami frequency band. *Natural Hazards and Earth System Sciences*, *6*(6), 1035–1051. https://doi.org/10.5194/nhess-6-1035-2006

Okal, E. A.; 2021: On the possibility of seismic recording of meteotsunamis. *Pure and Applied Geophysics*, *177*(8), 3989–4005. https://doi.org/10.1007/s00024-020-02495-8

Proudman, J.; 1929: The effects on the sea of changes in atmospheric pressure. *Geophysical Supplements to the Monthly Notices of the Royal Astronomical Society*, *2*(4), 197–209. https://doi.org/10.1111/j.1365-246X.1929.tb05408.x

Rabinovich, A. B.; 2009: Seiches and harbor oscillations. In Y. C. Kim (Ed.), *Handbook of Coastal and Ocean Engineering* (pp. 193–236). World Scientific. https://doi.org/10.1142/9789812819307_0005

Šepić, J., Vilibić, I., & Rabinovich, A. B.; 2012: Occurrence of meteotsunamis in the Adriatic Sea and their relationship with atmospheric processes. *Marine Geophysical Research*, *33*(2), 89–103. https://doi.org/10.1007/s11001-012-9155-9

Tojčić, I., Vilibić, I., Denamiel, C., & Šepić, J., 2021: Meteotsunami early warning system prototype for the Adriatic Sea. *Frontiers in Marine Science*, *8*, 632613. https://doi.org/10.3389/fmars.2021.632613

Vilibić, I., Denamiel, C., Zemunik, P., & Monserrat, S.; 2021: The Mediterranean and Black Sea meteotsunamis: An overview. *Natural Hazards*, *106*(1), 1223–1251.

Vilibić, I., Monserrat, S., Rabinovich, A. B., & Sytov, V. N.; 2008: Numerical modeling of the destructive meteotsunami of 15 June 2006 on the Balearic Islands. *Pure and Applied Geophysics*, *165*(11–12), 2169–2195. https://doi.org/10.1007/s00024-008-0426-5

Vilibić, I., Šepić, J., Rabinovich, A. B., & Monserrat, S.; 2016: Modern approaches in meteotsunami research and early warning. *Pure and Applied Geophysics*, *173*(12), 3893–3914. https://doi.org/10.1007/s00024-016-1354-6

Corresponding author: silviazappala@hotmail.it